$CD8^+$ T cell hyperfunction in advanced liver fibrosis murine model and its association with tumor growth

Jood Madani

University of Ottawa

in partial Fulfillment of the requirements for the

[Master of Science]

Microbiology and Immunology

Department of Biochemistry, Microbiology, and Immunology

Faculty of Medicine

University of Ottawa

ABSTRACT

Advanced liver fibrosis in chronic hepatitis C infection (HCV) is associated with a generalized impaired immune system. Many immune cells are affected in chronic liver disease, including $CD8^+$ T cells. The Crawley lab reported $CD8^+$ T cell hyperfunction in cirrhotic HCV-infected individuals that persisted after effective antiviral therapy. To evaluate the link between $CD8^+$ T cell dysfunction in advanced fibrosis, we adapted a hepatotoxic carbon tetrachloride (CCl_4) murine model. We consistently observed severe fibrosis in CCl_4-treated mice resembling fibrosis in chronic HCV infected individuals. After stimulation of PBMC, the proportion of granzyme B^+, and IFN-γ^+ $CD8^+$ T cells in fibrotic mice was significantly higher than the controls, particularly naïve and central memory $CD8^+$ T cells. This state of hyperfunction was sustained after liver insult removal and significant fibrosis regression to near normal tissue integrity. Sex differences were also studied in this model and were apparent after prolonged exposure to CCl_4 and in the capacity to repair liver fibrosis. Following an ectopic challenge with cancer cells, tumor growth was significantly greater in fibrotic mice. Moreover, the response to immunotherapy was significantly delayed in CCl_4-treated mice. In summary, we reported for the first time that circulating $CD8^+$ T cells are hyperfunctional in a murine model of advanced liver fibrosis in response to a hepatotoxin. In this context, affected mice failed to control the growth of a tumor whose growth is known to be controlled by a robust $CD8^+$ T cell response. In addition, the reduced responses to immunotherapeutic effects suggest deficiencies in antigen-specific $CD8^+$ T cell responses. Therefore, this animal model might be useful to identify mechanistic targets with translational potential for immune restoring treatments in human chronic liver diseases with advanced liver fibrosis.

ACKNOWLEDGMENTS

My deepest gratitude to my primary supervisor, Dr. Angela Crawley, who has been an incredible teacher and supervisor, helping me to improve my scientific research skills. She has provided and supported me in acquiring the necessary training and skills to be a good researcher and scientist. I am grateful for her support and for being the first to truly teach me how to be brave and complete all challenges during my studies, especially during a worldwide pandemic. Her advice, guidance, and encouragement to participate in local and international conferences and present my work to learn and receive great feedback from other scientists in the field was invaluable.

I would also like to thank my co-supervisor Dr. Michele Ardolino, without whom this project would not have been completed. I am grateful for him having initially welcomed me to the graduate studies program as it was instrumental in establishing the collaboration with Dr. Crawley. I am grateful for his cooperation in one-on-one instruction with data analysis, patiently training me to be independent in this project. His intellectual contributions to the study as well as the provision of sharing the costs of supplies including animals, cell lines and antibodies that were required to complete all conducted studies in this project is much appreciated.

I would also like to thank my thesis advisory committee members, Dr. Barbara Vanderhyden and Dr. Erin Mulvihill for their guidance during my MSc research journey. They were incredible and supportive advisors who guided me to improve my skills and complete this degree successfully.

I want to thank Dr. Agatha Vranjkovic and Dr. Mohamed Hasim Shaad. They were the milestones for this project by conducting and participating in the initial optimization of the

model. I appreciate how they trained and mentored me when I started working in the lab and supported me with the animal work. Also, I would like to thank Jeff Li, a MSc-PhD student in the Crawley lab who participated in a large-scale animal experiment in progress during the research shutdown due to the pandemic. I enjoyed working with him and all lab members, who have provided a friendly working environment.

Lastly, I would like to thank my mother, father, twin brother, husband, and the rest of my family, without whom I would not have been able to complete this degree. I appreciate all the encouragement and support which allowed me to cope with many challenges and made it possible to finish this thesis while I studied overseas, especially during the pandemic.

LIST OF ABBREVIATIONS

APC – Antigen-presenting cell

CCl_4 – Carbon tetrachloride

CMV – Cytomegalovirus

CTL – Cytotoxic T lymphocyte

DAA – Direct-acting antiviral

DC – Dendritic cells

EBV – Epstein-Barr virus

GrzB – Granzyme B

HBV – Hepatitis B virus

HCC – Hepatocellular carcinoma

HCV – Hepatitis C virus

HFD – High fat diet

HIV – Human immunodeficiency virus

HSC – Hepatic stellate cells

IFN-γ – Interferon-gamma

IL – Interleukin

ISG – IFN-stimulated genes

KC – Kupffer

KP – Kilopascal

LCMV – Lymphocytic choriomeningitis virus

LSEC – Liver sinusoidal endothelial cells

NAFLD – Non-alcoholic fatty liver disease

NASH – Non-alcoholic steatohepatitis

NK –Natural killer

NKG2D – Natural killer group 2D

NKT – natural killer T cells

PD-1 – Programmed cell death protein

SVR – Sustained virologic response

TCR– T-cell receptor

TGF-β –Transforming growth factor beta

TNF-α – Tumor necrosis factor-alpha

LIST OF FIGURES

Table of Contents

CHAPTER 1: INTRODUCTION

1.1. The burden of chronic liver diseases

There are many liver diseases that can be caused by metabolic disorders, alcohol consumption, viral hepatic infections, or cancer. The incidence of these diseases is on the rise, and globally, the most common liver disease is non-alcoholic fatty liver disease (NAFLD). The prevalence of NAFLD is increasing worldwide. It currently affects≈25% of the world population[120,] at approximately: 30% in the Middle East and South America, ≈24-27% in North America, Europe, and Asia, and 13% in Africa, and it continues to increase[120]. This increased prevalence of NAFLD has been reported in all age and racial groups[47]. High caloric intake, obesity, metabolic syndrome, insulin resistance, and/or type 2 diabetes are the most common causes of NAFLD. NAFLD is a silent disease that progresses slowly over ≈ 20 years and may lead to cirrhosis. Approximately 20-30% of NAFLD patients develop more complicated liver diseases such as non-alcoholic steatohepatitis (NASH)[48], which develops more rapidly, and 30% of those are more likely to develop cirrhosis[119] and end-stage liver disease[75]. Viral hepatitis is the leading infectious cause of chronic liver disease, mainly caused by the hepatitis B virus (HBV) or the hepatitis C virus (HCV). According to the World Health Organization, it is estimated that approximately 257 million and 71 million people worldwide are living with chronic HBV and HCV, respectively. Many HCV-infected individuals have now experienced sustained virologic clearance with the use of effective direct-acting antivirals and the incidence of HBV infections has been reduced with vaccination where accessible. However, many people who are infected still remain at-risk of negative health outcomes associated with chronic liver diseases such as portal hypertension, end-stage liver disease, hepatocellular carcinoma (HCC), extrahepatic cancers, liver transplant, and susceptibility to re/co-infection.

In 2013, the prevalence of NAFLD-related HCC was 4-22% worldwide[75]. Since then, it has been shown that the prevalence of NASH-related HCC in patients with HBV or HCV infections is on the rise as NAFLD cases continue to rise evermore[88,82,6,98]. In Canada, the prevalence of chronic liver diseases has risen from one in ten to one in four in a decade, suggesting ≈7 million Canadians have a form of liver disease (as reported by the Canadian Liver Foundation), and it is estimated this will increase by 20% between 2019 and 2030[101]. According to the Public Health Agency of Canada, ~ 600,000 individuals are currently infected in Canada with HBV and/or HCV, and mortality from viral hepatitis and liver cancer is increasing dramatically[14].

1.2. Healthy liver function

The liver is located in the right upper quadrant of the abdomen and plays an integral role in the functioning of other organs of the digestive system such as the gallbladder, pancreas, and intestines, by filtering all blood for substances that pass through the stomach and enter the liver via the portal vein[46]. The liver is the largest solid organ in the body and plays a vital role in the health of the host, and unlike other solid organs, it has the capacity to completely regenerate itself[66]. It has a unique anatomical architecture with several types of cells that perform many hepatic functions that are mainly (≈ 60-80%) composed of parenchymal cells, hepatocytes, which are the primary epithelial cells of the liver and perform most of its metabolic functions. Non- parenchymal cells constitute ≈ 20-40% of the total cell population of the liver, including endothelial cells (50%), the second major cell type in the liver, Kupffer cells (20%), lymphocytes (25%), biliary (5%), and stellate (<1%) cells[10,86]. Liver sinusoidal endothelial cells (LSECs) are essential cell populations that have an important role both

metabolically and immunologically in the liver[81,15]. The liver has four main functions in the body: metabolic, immunological, vascular, and secretory/excretory[68].

1.3. Monitoring liver disease severity

There are several clinical practices that are used as the standard of care for diagnosing and staging liver pathology and function. An elevation in the level of liver enzymes is the most common diagnostic practice used clinically as an initial red flag to diagnose any existence of liver damage[31,99]. Tissue imaging by ultrasound elastography (e.g.Fibro-scan) can be used to determine the extent of liver scarring based on measurements of liver thickness. This has largely replaced liver biopsy collection as the standard of care for HCV-infected individuals[23]. Serum biomarkers are increasingly being used as an additional non-invasive alternative tool to detect fibrosis progression in measuring the aspartate aminotransferase/platelet ratio index (APRI) and the Fibrosis-4 (FIB-4) index[112]. However, the cut-offs of liver fibrosis severity using these biomarkers vary depending on the liver etiology[56,53]. Extracellular vesicles (EVs) such as exosomes, microvesicles, and apoptotic particles are under investigation as potential biomarkers of liver disease progression[96,69,11]. However, there are inherent limitations in the usage of biomarkers to determine liver fibrosis severity compared to the direct evidence afforded by biopsies[107].

Isolated core needle biopsies for histopathological assessment of liver tissue have long been standard for diagnosing and staging liver disease and detecting liver cancer. Microscopic evaluation of structural anatomy at the cellular level by either light or electron microscopy can identify and diagnose liver disease in mice and humans by a trained pathologist. Tissue section staining further aids histological observations, so when the biopsy is collected with a core needle, the connective tissue can be readily seen by histological staining with Masson's

trichrome or reticulin[23]. Such staining shows the patterns of tissue damage such as fibrosis, inflammatory staging, and connective tissue deposition, and it can also be used for diagnosis and progression of treatment. Histology is a critical and efficient technique that is widely employed for liver damage diagnosis. However, a liver biopsy is the last and least preferred method for liver diagnosis due to its invasiveness and associated procedural risks.

1.4. The liver as an immune organ

1.4.a. Immunologic function of the liver

The liver is a frontline immunological organ and plays an important role in innate and adaptive immunity. It has many resident cells of the innate and adaptive immune system, and immune cells repeatedly pass through the liver through circulation. When the blood enters the liver via the hepatic artery and portal vein, it might carry a potential pathogen[51]. Unlike the slow response of adaptive immunity, the liver as an innate immune organ responds quickly to any foreign particle entering through flowing blood. The role of the liver's hepatic immune responses to detect and protect the host from a bacterial and viral infection when a foreign particle enters through the gut has been previously studied[27]. Hepatic sinusoid cell populations include endothelial cells, resident macrophages, Kupffer cells (KCs)[122,45], resident natural killer cells (NKs) cells, dendritic cells (DCs), and fat-storing cells[36]. The contribution of these innate immune cells in the liver includes enhancing the body's resistance to infection in producing acute phase proteins, nonspecific phagocytosis by KCs, killing of pathogen-infected cells by NKs, and pinocytosis of waste molecules such as collagens[80]. Adaptive immune cells in the liver participate in numerous immunological functions, such as the clearance of remaining activated T cells after inflammation subsides, the clearance of proliferative extrathymic T cells, the disposal of immune-mediated interaction waste, tolerance towards

self-antigens[80], and, finally, the activation of $CD8^+$ T cells by hepatocytes[122,85,10,18]. More importantly, T cells infiltrating the liver, particularly $CD8^+$ T cells, have a major role in the clearance of hepatic viral infections[97,80]. B cells also play a role in mediating T cell functions in the liver through cytokine secretion, regulatory functions, and inflammation[59-60].

1.4.b. Immune tolerance

It has been shown that hepatocytes play a critical role in capturing an antigen and mounting a robust immune response by activating liver resident lymphocytes; however, since the liver is receiving a third of the total blood volume, liver response is well maintained to inhibit a profound autoimmune reaction against any potential self-antigen molecules of oral food antigens or host-microbiota that enter through the gut. Specific cell-mediated immunity between the innate and adaptive immune cells is a highly regulated process. Recent studies suggest that as a tertiary lymphoid organ, the liver has a prominent role in the defence against harmful pathogens due to its well-organized innate immune system, involving hepatocytes that play a role in generating 80-90% of circulating acute-phase proteins[123,80]. Although many cells such as hepatocytes and endothelial cells can activate T cells by functioning as presenting antigen cells, they are minimized in the liver due to its very suppressive cellular and micro-environment, leading to premature T cell death and immune tolerance[37,32].

1.5. Chronic liver diseases and immune dysfunction

It is well documented that despite their aetiologies, chronic liver diseases significantly impact host immunity. This impact is observed on both innate and adaptive immunity. Several studies have shown immune dysfunction associated with liver diseases such as viral infections, cirrhosis, and HCC. However, there are fewer reports that connect immune dysfunction with

fibrosis severity, and dysfunctional immunity remains poorly understood in the context of liver fibrosis severity.

1.5.a. Non-alcoholic fatty liver disease (NAFLD)

NAFLD is the most common form of chronic liver disease. Fatty liver disease is strongly associated with obesity and insulin resistance[109,102]. Some cases are associated with widely prescribed pharmaceutical drugs such as amiodarone, tamoxifen, and glucocorticoids used to treat breast cancer, depression, heart diseases, and inflammatory and immunological disorders. NAFLD is a metabolic disorder described as hepatic steatosis based on the histological finding of fat depositions in the liver mediated by triglycerides or lipid droplets (over 5% of the liver weight). In the absence of other aetiologies, it can be more pronounced alongside of other aetiologies of hepatic diseases. NAFLD morphology is classified as macrovesicular, with large fat droplets displacing the nucleus and cellular organelles[35]. Simple steatosis is the first stage of liver disease that arises with acute chemical or drug exposure, and it regresses after liver insult removal. However, in 30% of NAFLD patients, steatosis progresses to inflammatory non-alcoholic steatohepatitis (NASH) with prolonged and significant liver injury and is classified morphologically by microvesicular and/or macrovesicular steatohepatitis[25,35,121,54]. Steatosis may also result in fibrosis progression to cirrhosis. It is not yet known the circumstances that lead to such progression.

1.5.b. Immune cells causing tissue damage

Both circulating and resident innate immune cells play a role in the pathogenesis and clearance of hepatic viral infections. The association between a dysfunctional immune system and NAFLD has been studied for decades. Some studies have linked immune cells to the

progression of NAFLD and NASH pathology. This occurs by involving many immune cells and their cytokine and chemokine production in activating hepatic stellate cells (HSC) and fibrogenesis[100]. Also, the involvement of innate immunity in NASH progression was shown to occur due to enhanced inflammation[105].

1.5.c. Effect of liver disease on the immune system

Other researchers have shown that fatty liver disease negatively impacts immune cell survival and function[63]. When the liver is injured, resting HSCs are activated, resulting in increased extracellular matrix components, including collagen (I and III). Then, the damaged hepatocytes and resident and non-resident immune cells start to release inflammatory chemokines and cytokines. The accumulated fatty acids is a pathological and functional feature of NAFLD that are metabolic changes lead to intrahepatic $CD4^+$ T cell death and accelerates HCC pathogenesis in mice and humans[65]. Multiple studies have shown the association between chronic liver diseases and systemic immunological dysfunction. These changes in immune function are associated with an environmental alteration in chronic liver diseases, resulting in dysfunctional immune cells. For instance, there is a significant change in the proportion of KCs, NK, and NKT cells in addition to an altered cytokine microenvironment locally and systemically; all of which are thought to contribute to liver disease progression in NAFLD, NASH, or HCC[50]. However, the association of liver fibrosis severity in non-infectious chronic liver disease on CD8+ T cells is less well understood.

1.5.d. HCV infection

The HCV virus is a double-enveloped, small (55-56nm), positive-sense, single-stranded RNA virus. It is a member of the Flaviviridae family, belonging to the genus

Hepacivirus, and a member of the species Hepacivirus C. Its envelope is well-structured and aids in its evasion of the immune system[57]. In the last few decades, seven genotypes of the HCV virus have been identified, defined as genotypes 1 - 7, and include 67 subtypes with global distributions[5]. The life cycle of the HCV virus involves four main steps to infect hepatocytes: cellular attachment and entry, translation, polyprotein processing, replication, and release from the infected cell. The process of HCV infection is complex and highly regulated via precise mechanisms; each step requires distinct host cellular machinery and viral factors[30,16]. While around 15-20% of those infected with the HCV virus can clear the infection spontaneously, over 80-85% develop chronic HCV infection. HCV transmission mainly occurs through blood-blood transmission, specifically via intravenous drug use, blood transfusion, other blood products, unsafe medical practices, perinatal and sexual transmission. The early symptoms of acute HCV infection are non-specific and not well characterized, so infected individuals often do not seek medical treatment. HCV infection is mostly asymptomatic (80% in infected individuals); however, ≈ 25% may develop some symptoms. The clinical outcomes of chronic HCV infection are metabolic liver disease, end-stage liver disease, liver cancer, reduced vaccination efficacy and liver transplant[30].

1.5.e. Current HCV Treatment

The standard treatment for chronic HCV^+ infection used to be pegylated-interferon alpha (PEG-IFN-α) or PEG-IFN-γ and ribavirin (RBV), achieving a sustained virologic response (SVR) rate of ~40-70%, depending on HCV genotype, within either 24 or 48 weeks of continuous treatment[30]. In 2011, direct-acting antiviral (DAA) therapy was officially licensed as an effective antiviral therapy for HCV infection and is now the standard of care in most developed countries. This treatment relies on blocking some of the HCV envelope

proteins or the serine protease complexes (NS3 and 4A) required for polyprotein cleavage steps[30,67,49]. The standard DAA medication is used alone, eliminating viral titers in blood and liver, with a 98% SVR efficacy across all HCV genotypes[87,94]. It was observed that innate immune cells contribute to HCV clearance with DAA therapy, showing an elevation in IFN responsiveness on peripheral NK cells in patients who achieved SVR compared to those who experienced a breakthrough infection[3]. DAA treatment-mediated HCV clearance decreases expression of type II and III IFN-stimulated genes (ISGs) while partially restoring immune cell responses, particularly virus-specific $CD8^+$ T cell responses[87,115]. Liver fibrosis is the major consequence of HCV infection. Liver fibrosis progression in chronic HCV infection occurs very slowly within seven years; however, with ongoing liver insult, 16% of infected individuals with HCV can develop cirrhosis after 20 years of infection, with a risk of 41% developing cirrhosis after 30 years[103]. Nevertheless, fibrosis regression after DAA treatment is variable depending on liver stiffness measuring in Kilopascals (KPa), age, and duration of the infection. For example, HCV^+ individuals with F2/3 fibrosis may revert almost fully to F1, but they might not if they are cirrhotic, particularly those with the highest kPa damage[48,103].

1.5.f. Impaired immune functions in HCV infection

Chronic liver disease significantly affects immune responses, impairing cells of both the innate and adaptive immune system. Since most acute-HCV infected individuals are asymptomatic, the innate immune responses to an early phase of HCV infection were studied in a chimpanzee model[78]. In the first few days post-HCV-infection, the expression of ISGs were significantly elevated, particularly among innate immune cells. Weak type I IFN responses, and low titers of virus-neutralizing antibodies are the most observed signs in acute HCV infection, and the involvement of adaptive immune responses takes between 8-12 weeks

to clear the infection in chimpanzee models, or they develop chronic infection[79,3]. Similarly, HCV-infected individuals who cannot clear the infection spontaneously by 12 weeks post-infection are more likely to develop chronic HCV infection, confirmed with persistent viremia[78,104]. Many reports have shown the impact of HCV infection on immune cells such as macrophages, NKs, and DCs. Also, the dysfunctional and altered phenotype of virus-specific $CD4^+$ T cells[95] and impairment of terminally exhausted $CD8^+$ T cells have been widely reported[114].

$CD8^+$ T cells are affected significantly during acute and chronic HBV and HCV infections. For instance, many studies have shown that individuals with self-limiting HCV infection have an effective HCV-specific CD8 T cell response, whereas impaired and exhausted HCV-specific $CD8^+$ T cells are a hallmark of chronic HCV[108]. The exhaustion of $CD8^+$ T cells in HCV infection is observed in both bulk (generalized) or virus-specific T cells, identified by an increased expression of programmed cell death protein (PD-1) and, reduced interleukin-7 receptor α (CD127) expression[115]. HCV-specific $CD8^+$ T cell dysfunction in patients with chronic HCV infection was marked by impaired perforin induction and granzyme B expression[74]. In contrast, bulk $CD8^+$ T cells showed a hypersensitivity in chronic HCV and HBV infections, particularly naïve $CD8^+$ T cells. These immature $CD8^+$ T cells were hypersensitive to TCR signalling during chronic viral disease[2,12,111].

1.6. Cytotoxic CD8 T cells

$CD8^+$ T cells are an essential part of adaptive immunity, playing a critical role in the defense against hepatic viruses, other intracellular pathogens, or cancer. The major mechanisms of cytotoxic T lymphocytes (CTL) $CD8^+$ T cells used to kill infected or abnormal

cells via the secretion of pro-inflammatory and immunomodulatory tumor necrosis factor-alpha (TNF-α), interferon-gamma IFN-γ cytokines during viral infection, and the destruction of targeted cells by apoptosis mediated by cytotoxic granules such as perforin and granzymes as well as Fas/FasL or TNF-α death receptor signalling[110].

1.6.a. $CD8^+$ T cell functions

Upon antigen recognition by naïve T cells in lymphoid tissue, differentiated effector T cells express high levels of adhesion molecules and chemokine receptors displayed on infected cells. When effector $CD8^+$ T cells recognize class I MHC-peptides, they bind to infected cells and kill them by using several mechanisms, such as inducing apoptosis by exocytosis of CTL's granule proteins (granzymes, perforin, and TNF-α). Cytotoxic $CD8^+$ T cells also release granzymes into the cytoplasm of targeted cells, activating caspases which induce apoptosis. Perforin protein facilitates the delivery of granules by making pores on the membranes of infected cells. $CD8^+$ CTLs can also induce apoptosis by binding Fas ligands to death receptors to activate caspases in the cytoplasm of targeted cells. Secretion of the cytokine TNF-α is another mechanisms by which effector $CD8^+$ T cells destroy cellular targets in order to eliminate viral infection, and increase immune cell recruitment.

1.6.b. CD8 T cell exhaustion

$CD8^+$ T cell exhaustion was extensively studied in the chronic lymphocytic choriomeningitis virus (LCMV) mouse model in comparison with acute infections. In the acute phase of LCMV infection, naïve T cells undergo proliferation, clonal expansion, and differentiation into effector T cells. Typically, most effector cells die after viral clearance except a small subpopulation that differentiates into long-lived memory T cells. Each of those

subsets has a distinct epigenetic and transcriptional profile, depending on the status of the infection. Memory $CD8^+$ T cells are cytotoxic polyfunctional $CD8^+$ T cells, marked by elevated inducible cytokines, e.g., Interleukin (IL)-2, IFN-γ, and TNF-α. Those long-lived memory T cells are non-apoptotic, proliferative, and increase CTL receptors and survival capacity without antigens. However, with persistent antigen stimulation, effector T cells become exhausted, thereby losing their killing function and failing to differentiate into memory T cells. Antigen-specific T cell exhaustion is defined by increased apoptosis, reduced proliferation capacity, and lower cytokine secretion such as IL-2, IFNγ, and TNFα. T cell exhaustion is observed in chronic diseases such as HIV, HCV, and HBV[33,34,64,44]. Exhaustion of $CD8^+$ T cells can be determined by limited proliferation, upregulated ectonucleotidase CD39, altered transcriptional programs epigenetic profiles, altered expression of co-inhibitory molecules such as IL-10, and, finally, transforming growth factor beta (TGF-β)[114]. In addition, elevation in the expression of PD-1 on $CD8^+$ T cells is a hallmark of exhaustion in chronic illness and unregulated expression of CD127 on peripheral, chronic HCV-specific CD8 T cells[108]. It has been shown in Crawley's lab that generalized impairment of $CD8^+$ T cells in response to IL-7 stimulation in chronic hepatitis C virus infection, and the production of Bcl-2 signaling is related to the degree of liver fibrosis[92].

1.6.c. $CD8^+$ T cell hyperfunction

Development of chronic disease can lead to aberrant adaptive immune activation. Generalized hyperfunction of immune cells is observed in chronic infectious diseases with persistent pathogen burden such as HCV[2] and HIV[9], resulting in persistent antigen stimulation, leading to abnormal function of B and T lymphocytes. Non-specific T cell activation was observed a decade ago, defined by upregulated cytokine production in HIV

infection[58]. In addition to the general decline in $CD4^+$ T cell numbers in chronic HIV infection, hyperfunction of T cells was also observed as a hallmark of persistent antigen activation and ongoing systemic inflammation. This hyperfunction of T cells was associated with increased T cell apoptosis, viral load, and increased activation marker expression during disease progression. These associations with T cell hyperfunction were only observed in a small proportion of $CD8^+$ T cells and found mostly in activated HIV-specific or non-HIV-specific $CD4^+$ T cells in untreated individuals [34]. Another report observed hyperfunctional T cells in untreated HIV-infected patients, particularly in $CD8^+$ T cells. This hyperfunction was observed in both HIV-specific and non-HIV-specific T-cell responses to cytomegalovirus (CMV), Epstein-Barr virus (EBV), adenovirus, and influenza), marked by significantly increased production of IFN-γ and TNF-α on non-HIV-specific cells, associated with independent activation of $CD8^+$ T cells after HIV-1 rebound[9].

The hyperfunction phenomenon of T cells with persistent antigen activation was further explored in chronic HCV infection. Chronic HCV infection alters circulating $CD8^+$ T cells, resulting in hypersensitivity of naïve $CD8^+$ T cells in response to TCR stimulation[2]. In naïve T cells, this was marked by reduced CD5 protein expression on the cell surface, a significant induction of p-ERK (phosphorylation patterns involved in differential responses), as well as elevation in activation markers CD25 and CD96 in chronic HCV infection. Also, there was a hyperreactive pre-immune repertoire on memory cells and an increase in the expression of granzyme B and IFN-γ on antigen-specific $CD8^+$ T cells in response to different peptides (Mart-1, hTERT, CMV). In addition, this hyperactivation of immune cells was reported in association with advanced liver staging and cirrhosis, which are associated with adverse effects on the host immune system. It compromises the immune surveillance function

of the liver and more generally damages the function of peripheral and mucosal immune cells, when cirrhosis progresses from compensated to decompensated, leading to cirrhosis-associated immune dysfunction. Immune cells play a role in cirrhosis progression either by mediating hepatocyte damage and/or impairing by progressive advanced liver fibrosis. Cirrhosis induces a general state of immunodeficiency and systemic inflammation derived from the disturbance of several crucial functions both hepatically and systemically. For T lymphocytes, cirrhosis causes upregulated co/stimulatory marker expression, increased persistent activated state, increased systemic pro-inflammatory cytokine concentrations, reduced proliferation, and reduced antigen dependent responses due to persisting stimulation of immune cells[4].

1.7. Advanced liver fibrosis models

Mouse models are a useful tool for the study of liver fibrosis development. In the last few decades, many rodent models were developed for fibrosis research to mimic the clinical condition across aetiologies. These models can also help in the study of the pathogenic mechanisms of liver injury and advance the investigation of cellular and molecular interactions in liver disease. There are many ways to induce fibrosis in mice with hepatotoxins or high-fat diet (HFD) genetic models. The hepatotoxin carbon tetrachloride (CCl_4) can induce liver fibrosis. CCl_4 affects hepatocytes when metabolized by cytochrome P450 enzymes to the noxious trichloromethyl radical (CCl_{3-}), disrupting the permeability of plasma, lysosomal and mitochondrial membranes. CCl_{3-} causes lipid peroxidation and membrane alteration leading to centrilobular hepatocyte necrosis[93]. After the first injection of CCl_4, acute and centrilobular hepatocyte necrosis are observed. This is followed by the proliferation of hepatocytes and nonparenchymal liver cells, whose fibrotic effects can be observed after a few injections. Of

note, CCl_4-induced fibrosis can impact immune cells such as $CD8^+$ T cells, $CD4^+$ T cells, natural killer cells (NK), natural killer T cells (NKT), and B cells. According to a previous study, there was a slight increase in KCs and NK cells in CCl_4-induced fibrosis in mice. Intrahepatic $CD8^+$ T cell numbers increased two-fold in fibrotic mice, while IFN-γ production decreased, compared to the control group.

1.8. Sex effects in liver fibrosis

Although sex effects in liver fibrosis are still poorly understood, some studies have reported sex differences in liver diseases such as NAFLD[91], HBV[38], HCV[52,8], and in HCC[117,89]. Multiple studies have reported that the risk of liver fibrosis progression in HCV infection in women is ten times less than in men[83]. On the other hand, a recent report showed little difference in the NAFLD progression in males and females (36% and 31%) in young people and (64% and 63%) in adults, respectively[106]. Thus, a consideration of sex effects in the design of liver fibrosis studies is likely necessary.

1.9. Rationale and Hypothesis

There is a generalized impairment of $CD8^+$ T cells in chronic liver diseases. Our lab reported an association between dysfunctional $CD8^+$ T cells and liver fibrosis severity for the first time. Bcl-2, an anti-apoptotic molecule, decreased with HCV-infected individuals with advanced liver fibrosis (F3, F4) compared to those with minimal fibrosis (F1, F2)[92]. The Crawley lab then found that $CD8^+$ T cells were more hyperfunctional in HCV-infected individuals with advanced liver fibrosis than individuals with minimal liver fibrosis. This hyperfunctionality is characterized by increased secretion of perforin and degranulation of CD107a, and IFN-γ on $CD8^+$ T cells in HCV-infected individuals with advanced liver fibrosis.

These hyper-activate $CD8^+$ T cells in individuals with advanced liver fibrosis were sustained after clearing the infection with direct-acting antiviral (DAA) medication[111]. There is an increase in liver cancer risk in humans with advanced liver fibrosis. Given the critical role of $CD8^+$ T cells in anti-tumor responses, we will complement $CD8^+$ T cell dysfunction studies in liver fibrosis to assess responses to cancer challenges in our model. We hypothesized that **$CD8^+$ T cells are dysfunctional in a murine model of advanced liver fibrosis, promoting cancer development.**

1.10. Objectives

1- To determine the establishment of liver fibrosis in a murine model.

2- To assess $CD8^+$ cell function in liver fibrosis.

3- To assess response to cancer challenge in mice with liver fibrosis.

CHAPTER 2: METHODS AND MATERIALS

2.1. Animals:

This project follows an approved animal use protocol #3003 with the Animal Care Veterinary Services, University of Ottawa, certified by the Canadian Council on Animal Care (CCAC). A total of 138 C57BL/6 mice were purchased from the Jackson laboratory and used in this thesis research in six independent experiments. Sixty-seven mice were female and 51 male. Experiments were started when the mice were 8-11 weeks old.

Table 1: Conducted studies of advanced liver fibrosis in a murine model

Study*	Number of Mice	Sex	CCl_4 Treatment	Blood collection	Study questions
A	20	F	10 weeks	weeks 6,9,10	Fibrosis scoring (weeks8,10) $CD8^+$ T cell functions (weeks6,9,10)**
B	40	F	16 weeks	week 12	Fibrosis scoring (weeks12, 16) $CD8^+$ T cell functions (week 12) CCl_4 cessation (week 12) Response to a tumor (week 12) Response to immune therapy
C	18	11 M 7 F	19 weeks	weeks 0,4,8,12	$CD8^+$ T cell functions overtime*** Response to a tumor (week 12)
D	12	M	9 weeks	weeks 0,4,9	$CD8^+$ T cell functions over time
E	40	20 M 20 F	26 weeks	weeks 0,4,19, 21	$CD8^+$ T cell functions over time CCl_4 cessation (week 16) Response to a tumor (week 21)
F	8	M	12 weeks	weeks 0, 4, 8,12	$CD8^+$ T cell functions over time Response to a tumor (week 14)

*Study start dates **A**: Sep 2018; **B**: Dec 2018; **C**: June 2019; **D**: Sep 2019; **E**: Feb 2020, **F**: Feb 2021.

** Optimizing *in vitro* stimulation of $CD8^+$ T cells: time course, conditions, titration etc.

*** $CD8^+$ T cell function over time (≈weeks 0, 4, 8,12, etc.)

2.2. Hepatotoxin (CCl_4) administration in mice

To induce liver fibrosis in a murine model, we injected C57BL/6 mice, from the Jackson Laboratory, (≈ 11 weeks old) with a hepatotoxin. Bodyweight and physical condition were monitored twice weekly before each injection (Fig. 1). Mice were injected intra-peritoneally (i.p.) with either 1.0 ml/kg of carbon tetrachloride 99.9% (CCl_4) (Sigma-Aldrich, USA) diluted to 50% in filtered (0.45 nm) olive oil (Bertolli oil, as CCl_4 is hydrophobic) or only olive oil for the control group, twice a week for up to 12-16 weeks (Fig. 2A).

2.3. Liver collection

Mouse livers were collected from both study groups at different time points (weeks 4, 8, 12, 16), depending on the study. Collected livers were fixed with 10% formalin, shaken gently for 72 hours, transferred to 70% ethanol at 4°C, then paraffin-embedded and sectioned (Louise Pelletier Histology Core, University of Ottawa). The slides were stained with Masson's Trichrome three-color stain for fibrosis scoring. Liver fibrosis severity was assessed by an expert pathologist (Nour Histopathology Consultation Services, Ottawa, ON, Canada), blinded to the sample identities and treatments. Scoring followed the Metavir system from no fibrosis (F0) to advanced fibrosis (F4), used in both humans and mice[116].

2.4. Blood collection and isolation of peripheral blood mononuclear collection PBMCs

Mouse blood was collected from the saphenous vein into Microvette tubes CB 300 (Fisher Scientific, CA, USA) which contained the anticoagulant lithium heparin, and then transferred to 1ml of red blood cell (RBC) lysing buffer (Hypri-Max RBC lysing buffer, Sigma, Aldrich, USA) to collect peripheral blood mononuclear cells (PBMCs). After fiveminutes, cells were

washed twice with phosphate buffered saline (PBS) and centrifuged at 1600 revolutions per minute (RPM) with the break on. PBMCs were counted by trypan blue dye exclusion and concentrated at $1x10^6$ cells/ml in complete RPMI (supplemented with 20% FBS + Penicillin/Streptomycin).

2.5. Stimulating $CD8^+$ T cells *in vitro*

A high binding plate (Sarstedt, USA) was coated with CD3 antibodies (5ug/mL, clone: 145-2cll, BD Pharmingen, BD Biosciences, San Diego, CA, USA) in PBS and incubated for one hour at 37°C. After washing the wells with PBS, cells were added and supplemented with anti-CD28 antibodies (2ug/mL, clone: 37.51, BD Pharmingen, BD Biosciences, San Diego, CA, USA) for 48hr at 37°C.

2.6. Flow cytometry analysis of CD8+ T cell phenotype and function

2.6.a. Extracellular staining for $CD8^+$ T cells phenotyping

In the final six hours of cell culture, Brefeldin (Golgi plug, BD Biosciences, San Diego, CA, USA) and Monensin (golgi stop, BD Biosciences, San Diego, CA, USA) were added to inhibit protein transport. At this step, CD107a antibodies (APC, clone: 1D4B, Biolegend, San Diego, CA, USA) were also added. After six hours, cells were transferred to a V-bottom plate (Thermo scientific, USA) and washed once with PBS. Dead cells were labelled with the cell membrane permeating Zombie NIR (APC-Cy7, Biolegend, San Diego, CA, USA), a fixable viability kit (0.2:100 ul in PBS) for 30 minutes. Then, cells were washed with PBS Mouse Fc block (clone: 2.4G2, BD Pharmingen, BD Biosciences, San Diego, CA, USA) and added to PBMCs for 20 minutes in the dark at 4°C to block non-specific antigen binding. To assess $CD8^+$ T cells phenotypes, PBMCs were labeled with a cocktail of fluorochrome-conjugated anti-mouse

antibodies diluted in PBS/BSA (1%) (50ul/ well) for 20-25 minutes in the dark at 4°C. This cocktail included antibodies specific for activation markers such as PD-1 and NKG2D and surface markers to identify $CD8^+$ T cell subsets: CD44 and CD62L. CD8 T cells were sub-gated as: naïve ($CD44^-$, $CD62L^+$), effector ($CD44^+$, $CD62L^-$), and memory ($CD44^+$, $CD62L^+$). The antibodies of the cell surface labeling cocktail were purchased from Biolegend (San Diego, CA, USA): CD3-BV-510 (clone 17A2), CD4-AF700 (clone GK1-5), CD8a-BV785 (clone 53-6.7), CD19-Pe-Cy5 (clone 6D5), CD107a-APC (clone 1D4B), CD44-BV241 (clone IM7), CD62L-PE (clone MEL-14), PD-1-PE-Cy7 (clone 29F.1A12), or from Horizon, BD Biosciences (San Diego, CA, USA): NKG2D-BV711 (clone CX5).

2.6.b. Intracellular staining of $CD8^+$ T cells

After the surface labeling, cells were fixed and permeabilized according to manufacturer instructions (BD Biosciences San Diego, CA, USA): 100 ul/well of fix and perm buffer for 15 minutes, followed by washing with PBS/BSA (1%) for intracellular staining. To measure $CD8^+$ T cell function, intracellular antibodies for TNF-α (FITC, clone MAb11), IFN-γ^+ (BV650, clone 4S.B3) and granzyme-B (Texas red, clone GB11) (1 ul/ well each) were diluted in 1x perm wash buffer (100 ul/well) for 30 minutes. Cells were then washed with 1x perm wash, re-suspended in PBS/BSA (1%) 100 ul/well, and analyzed using a BD LSEFortessa™ flow cytometer.

2.7. Tumor implantation in mice

In 1975, the use of transplantable colon cancer was published in different strains of mice, specifically the adenocarcinoma MC38 cancer cell line. Since it is well known that $CD8^+$ T cells regulate tumor growth, we challenged the CCl_4-induced fibrosis model with the MC38

cancer cell line and anti-CTLA-4 and anti-PD-1 antibody-based immunotherapy to assess CD8 T cell responses to tumor growth. An evaluation of cancer development *in vivo* is a test of $CD8^+$ T cell function in liver fibrosis. $CD8^+$ T cell anti-tumor responses principally resolve responses to ectopic cancers derived from MC38 cells. This cancer model is also responsive to some degree to the effects of immunotherapy. Thus, we developed a murine model of liver fibrosis to study further the impact of chronic liver disease on the immune system, particularly $CD8^+$ T cells. Furthermore, the model will help explore the responsiveness of immune cells to tumor growth *in vivo*.

2.7.a. Assessing tumor growth *in vivo*

To examine $CD8^+$ T cell responses to an ectopic cancer *in vivo*, the control and CCl_4-treated mice were challenged with a colon adenocarcinoma cell line (MC38) (from Michele Ardolino), derived from C57BL/6 mice. MC38 cells were expanded *in vitro* in DMEM supplemented with 10% FBS one week or two weeks prior to *in vivo* injection to achieve culture confluency. Tumor cells were implanted subcutaneously in the left flank of the abdomen with $1x10^5$, $3x10^5$ or $1x10^6$ cells in 100 ul PBS, depending on the study. Once palpable, ectopic tumor growth was measured (length x width x height x 0.52) with a caliper every two days until the mice reached a humane end point (i.e. tumor reached 15 mm in diameter, animals were in distress, or tumor ulceration was observed, whichever came first). Tumor growth assessment occurred in tandem with twice weekly oil treatment (control), ongoing CCl_4 treatment or following CCl_4 cessation, depending on the study.

2.7.b. Assessing the effect of immunotherapy on tumor growth

In study B, when tumors volume reached approximately 75mm[3,90,43] mice were injected with checkpoint inhibitors (anti-PD1 + anti-CTLA-4 antibodies) (from Leinco) 200 ug of each ab/ injection every two days, three injections in total. Tumor outgrowth was monitored as described above.

2.8. Data Analysis

Flow cytometry data were analyzed using FlowJo 10.6 software (Tristar, USA). Graphs and statistics were generated using GraphPad Prism 7.0 software (San Diego, San Jose, USA). Data are presented as means $\pm$ standard deviation (SD), and statistical analyses were conducted by paired or unpaired two tailed Student's *t*-test, one-way ANOVA followed by Dunnett's post-test or two-way ANOVA as appropriate. $p<0.05$ was considered statistically significant.

CHAPTER 3: RESULTS

3.1. Monitoring the effect of CCl_4 treatment on mouse growth and health

Mice were injected i.p. with either olive oil (controls) or the hepatotoxin CCl_4 (1.0 ml/kg in olive oil) for up to 12 weeks to induce advanced liver fibrosis[55,93]. Previous studies have noted transient effects on body weight of i.p. CCl_4 treatment in rodents[28,24]. In all studies conducted here, mouse body weight was measured twice per week to monitor mouse health before injection. Mice receiving CCl_4 did not lose weight (Fig. 1). Rather, mice gained weight compared to their control baseline throughout the protocol. Occasional significant drops in weight of CCl_4-treated mice were observed in the first two weeks of injections, but they were transient and did not reach statistical significance. Overall, the well-being of mice indicated no significant effects after CCl_4 exposure, and mice did not show any signs of distress except a slight drop in body weight within 72 hours of CCl_4 exposure. This was noted consistently in all six independent studies that were conducted in this project (Fig. 1).

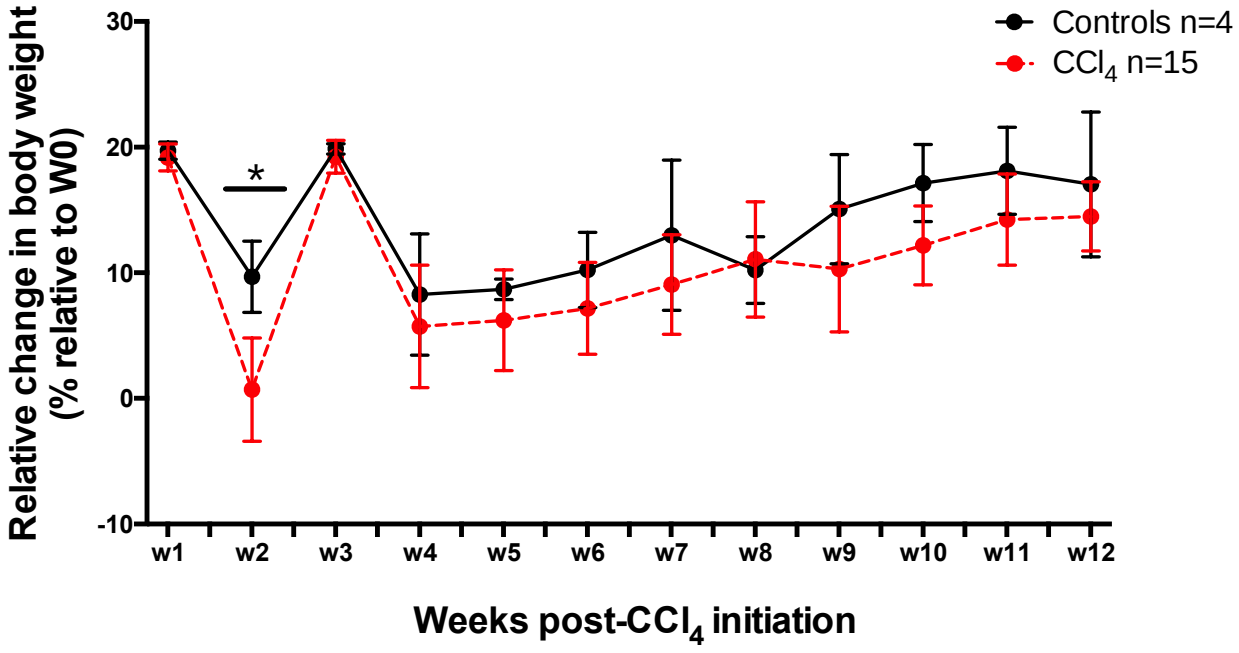
Controls n=4
CCl4 n=15
Relative change in body weight
(% relative to W0)
30
20
10
0
-10
*
w1
w2
w3
w4
w5
w6
w7
w8
w9
w10
w11
w12
Weeks post-CCl4 initiation

Figure 1. No significant difference in body weight gain between control and CCl4-treated mice over time.

C57BL/6 mice were injected i.p. with either filtered olive oil alone (control, black) or 1 ml/kg body weight CCl_4 in filtered olive oil (red), twice a week for up to 12 weeks. Body weights were measured weekly and are expressed here as relative change (%), compared to weight at week 0, reflecting study E. Mouse weights are represented as group means ($\pm SD$). There was no statistically significant difference between the treated groups, as determined by the one-way ANOVA test. The experiment depicted is representative of six studies conducted with similar results.

3.2. CCl_4-induced advanced liver fibrosis in a mouse model

3.2.a. Liver fibrosis severity in CCl_4-treated mice

After administering the hepatotoxin CCl_4 in mice for ≈12-16 weeks, depending on the study, livers were collected, formalin-fixed, and paraffin-embedded, sectioned, and stained for the scoring of fibrosis by a pathologist. Masson's Trichrome staining is used selectively to distinguish between collagen fiber deposition in the liver (in blue) and other hepatic structure in the background such as hepatocytes, muscles, and fibrin (in red). As expected, histology images of control mice showed no detectable liver fibrosis (i.e. F0), or minimal fibrosis (F1) (Fig. 2B). In CCl_4- treated mice, fibrosis could be detected at weeks 4 and 7 post CCl_4, progression of minimal fibrosis detected (F1/F2), described as mild diffuse bridging fibrosis. With the continued CCl_4 treatment, mice exhibited progression to advanced liver fibrosis, with most scored at F3 (e.g. 3/5 mice in study B) across all six experiments by ≈12 weeks, characterized as bridging fibrosis with focal necrosis. Other CCl_4- treated mice were graded as F4, marked by severe diffuse thick fibrosis with focal necrosis and connected septa (Fig. 2C-E). These results were seen repeatedly in all independent studies, and no sex effect was observed (study B, C) (Fig. 2F). These results indicate that advanced liver fibrosis is consistently induced in C57BL/6 mice, following CCl_4 administration. Furthermore, mouse liver pathology resembled, in part, the same pathology observed in livers of HCV-infected patients[17], confirming the suitability of this murine model of advanced liver fibrosis.

A)

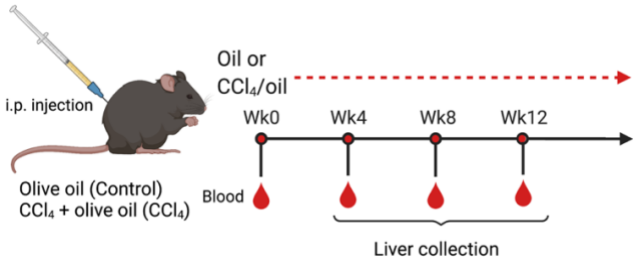
i.p. injection
Olive oil (Control)
CCl_4 + olive oil (CCl_4)
Oil or
CCl_4/oil
Wk0
Wk4
Wk8
Wk12
Blood
Liver collection

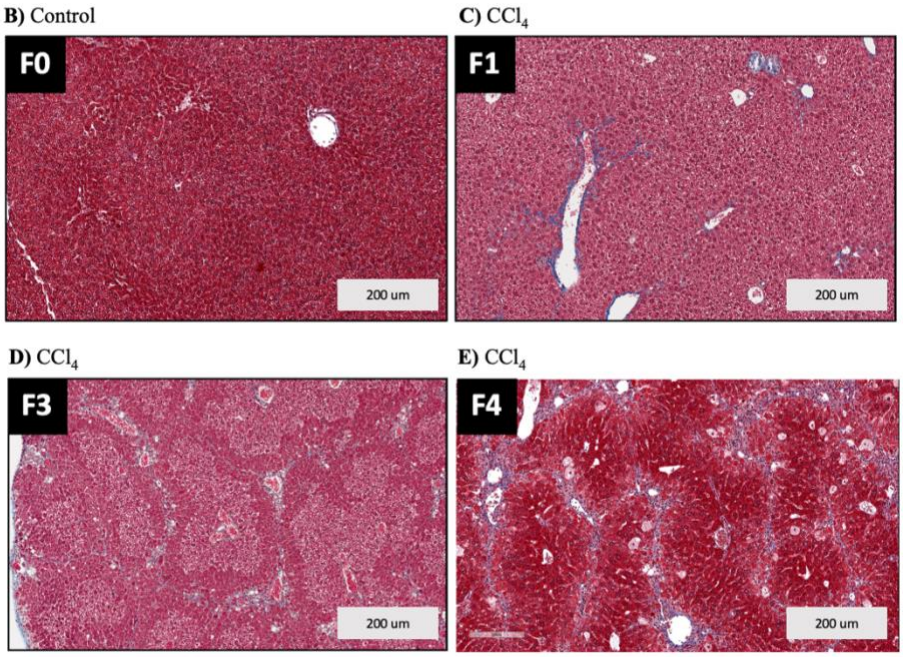
B) Control
C) CCl_4
D) CCl_4
E) CCl_4
F0
F1
F3
F4
200 um

F)

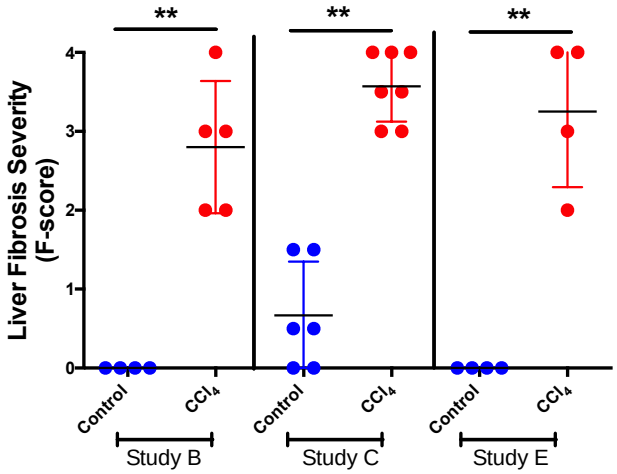
Liver Fibrosis Severity
(F-score)
**
**
**
Control
CCl_4
Study B
Study C
Study E

Figure 2. The hepatotoxin CCl4 induces advanced liver fibrosis in C57BL/6 mice.

A. Schematic experimental design of CCl_4 murine model of advanced liver fibrosis. Mice aged 9-11 weeks old (C57BL/6, weighing ≈18g for females and ≈25g for male) were injected intraperitoneally (i.p.) with either filtered olive oil alone for control or (1ml/kg body weight) CCl_4 in (3:1) filtered olive oil for treated mice, twice a week for up to ≈12-16 weeks. Blood was collected (saphenous) from both groups at the beginning of the experiment (week 0) and every four weeks during the treatment (weeks 4, 8, 12), to assess circulating $CD8^+$ T cell phenotype and functions. **B-E. Histology images show liver fibrosis severity.** Following euthanasian, livers were harvested from selected euthanized mice every four weeks to assess liver fibrosis progression during the treatment and to identify the peak of liver fibrosis. Liver fibrosis severity is indicated in the stages occurring to the Metavir (F-score) system: F0 = no fibrosis, F1/2 = minimal liver fibrosis, F3/4 = advanced fibrosis. Masson Trichrome three colors staining is represented by scanning microscopy at 10x magnification. When the pathologist reported fibrosis F0/F1 = (F0.5), F3/F4 = (F3.5). Representative images of collected tissue sections from livers from controls B) Control 12 weeks, and CCl_4-treated mice at **C)** 7 weeks; **D)** 10 weeks; **E)** 15 weeks. **F. A summary of liver fibrosis severity** scores for mice administrated oil or CCl_4 for 12-16 weeks is shown (studies B, C, E). Data are shown with group as means (±SD), and statistically significant differences were determined using a two-tailed unpaired Students' *t*-test (**$p<0.001$). This experimental design and histology staining were conducted repeatedly in all independent studies that were conducted in this project (Table 1)

3.1.b. Fibrosis regression in a liver fibrosis mouse model

To evaluate liver fibrosis regression, CCl_4 injections were ceased at the peak of fibrosis (typically ≈12 weeks post CCl_4 initiation, Fig. 3A). As shown in Table 1, we tested this in two independent studies (B, E, Table 1). In study B, no significant fibrosis was detected after 12-16 weeks of oil injections in control mice (n=11), with most scoring F0/1 (9/11 mice) and two scoring moderate fibrosis F2 (2/11 mice). The CCl_4-treated group, however, developed a significant amount of fibrosis compared to the oil control group at week 12 as shown in 3.1.A. By week 16, fibrosis severity significantly reversed to control levels (F1) (study B), while those mice that continued to be administered the hepatotoxin maintained tissue pathology consistent with advanced liver fibrosis (Fig. B-C). Nevertheless , in study B with only females, there was significant regression between week 12-16 (four weeks post cessation) scoring mostly F1 (3/4 mice) (Fig. 3D). More surprisingly, in terms of sex differences, fibrosis regression was more evident in male (F1) than female (F2) mice after CCl_4 cessation when CCl_4 was stopped at week 16 and assessed until mice were euthanized, depending on the end point of each mouse (week 24-30) (study E, Fig. 3E).

A)

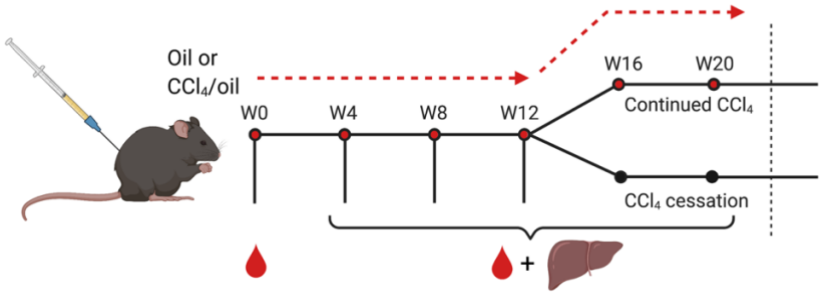

B) CCl_4 Cessation

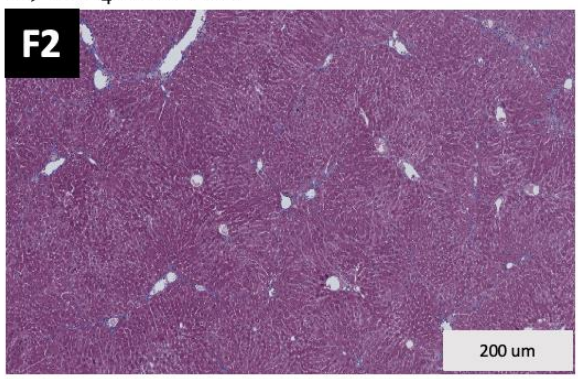

C) CCl_4 Continuation

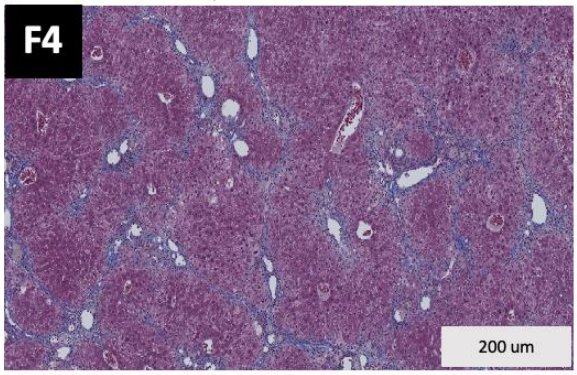

D)

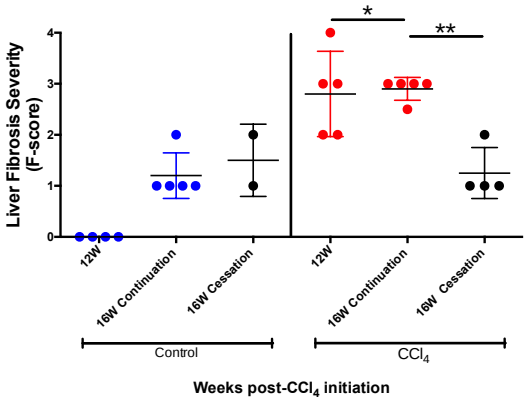

E)

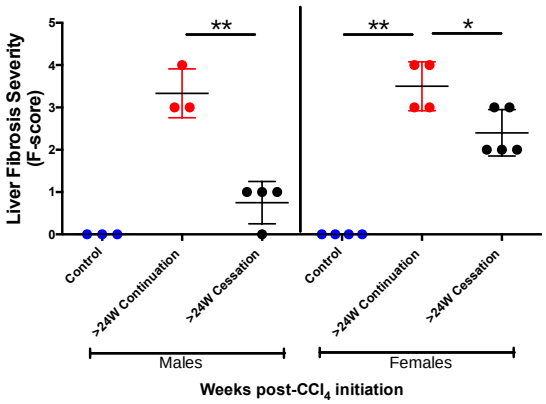

Figure 3. Fibrosis progression and regression in CCl4-treated mice.

A. Schematic experimental design of CCl_4 continuation and cessation in a murine model of liver fibrosis. C57BL/6 mice were injected (i.p.) twice a week with only filtered olive oil or 1ml/kg of the hepatotoxin CCl_4 in filtered olive oil for up to 16 or 20 weeks depending on the study, study B and E respectively. At week 12, the CCl_4 treated group was divided into two groups: one group continued to be administrated CCl_4, while CCl_4 treatment was stopped in the other group. This design was conducted in study B (n=40 female mice), and E (n=40 mice, 20 females and 20 males) to evaluate liver fibrosis regression. **B-C. histology images show liver fibrosis regression.** Liver fibrosis severity in CCl_4-treated mice eight weeks -post CCl_4 cessation or continuation. Masson Trichrome three color staining is represented by scanning microscopy at 10x magnification. **D. Liver fibrosis regression in CCl_4-hepatotoxin model in female.** In study B, CCl_4- treated mice continued CCl_4 treatment for an additional four weeks or CCl_4 treatment was stopped. The graph represents fibrosis severity of livers collected from these mice, compared to severity scores recorded at the peak of fibrosis (i.e. week 12), female mice (n=25, control=11, CCl_4-treated mice=14). From both groups, livers harvested for scoring at weeks 12 and 16, four weeks post-oil (blue) and CCl_4 (red) continuation or cessation (black). Data are presented as means ($\pm$SD), statistical significance between the two groups was determined using a two-tailed unpaired Students' *t*-test (*$p<0.05$ or **$p<0.001$). **E. fibrosis progression and regression in CCl_4-treated mice in males and females.** In male or female mice (study E), liver fibrosis was scored in oil control mice (blue) at week 12 and >24 weeks, post- CCl_4 continuation (red) or cessation (black), 24-32 weeks of treatment, (n=40, 20 males and 20 females. Data are presented as means ($\pm$SD), statistical significance between the two groups was determined using a two-tailed unpaired Students' *t*-test (*$p<0.05$ or **$p<0.001$).

3.2. Peripheral CD8+ T cell hyperfunction in advanced liver fibrosis

3.2.a. Induction of cytolytic molecules in advanced liver fibrosis

HCV-infected individuals with advanced liver fibrosis present bulk $CD8^+$ T hyperactivation (as assessed using the degranulation marker CD107a)[111].Therefore, we assessed if CCl_4-induced liver fibrosis also induced CD8 T cell hyperactivation. Blood was collected at peak liver fibrosis (≈week12), and PBMCs were stimulated with anti-CD3/28 for 48 hrs until CD8 T cells were assessed for CD107a expression. This stimulation significantly induced detectable CD107a in control mice. No differences were observed between control and CCl_4-treated mice in the proportion of $CD107a^+$ cells in circulating $CD8^+$ T cells with one exception, (study B) (Fig. 4C) where there was a significant reduction in the detection of $CD107a^+$ on bulk $CD8^+$ T cells in CCl_4-treated mice ($p<0.05$) (Fig. 4D). These results were seen in multiple experiments, indicating there were no changes in CD107a detection on bulk $CD8_+$ T cells in CCl_4-treated mice compared to the controls.

A)

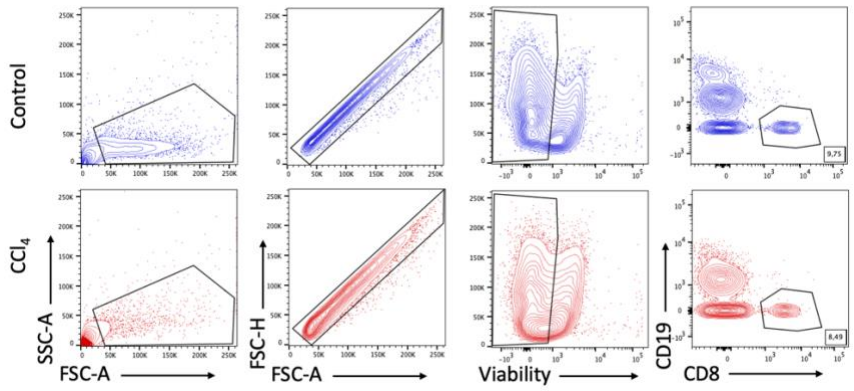
Control
CCl4
SSC-A
FSC-A
FSC-H
FSC-A
Viability
CD19
CD8

B)

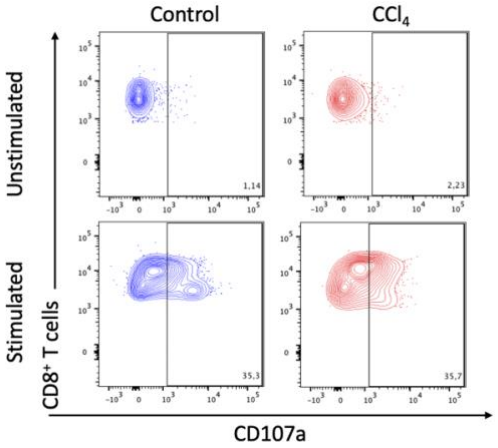
Control
CCl4
Unstimulated
Stimulated
CD8+ T cells
CD107a

C)

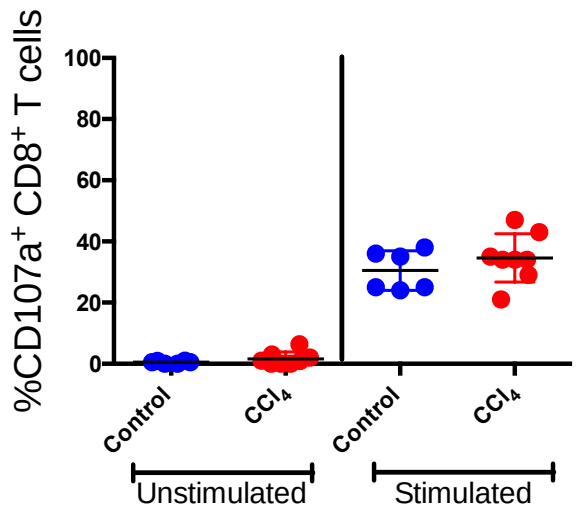
%CD107a+ CD8+ T cells
100
80
60
40
20
0
Control
CCl4
Control
CCl4
Unstimulated
Stimulated

D)

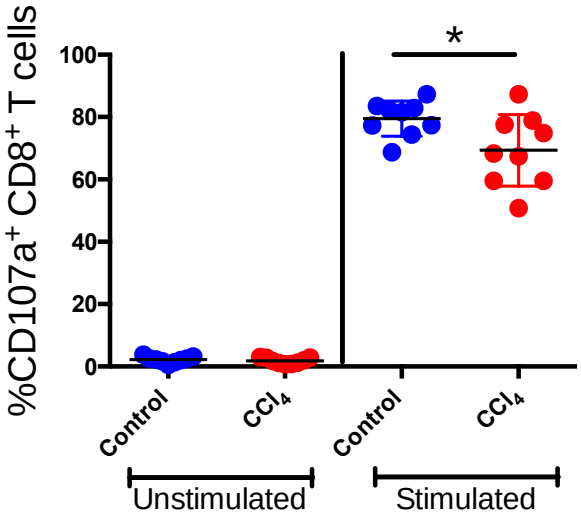
%CD107a+ CD8+ T cells
*
100
80
60
40
20
0
Control
CCl4
Control
CCl4
Unstimulated
Stimulated

Figure 4. The percentage of CD107a+ CD8+ T cells at the peak of advanced liver fibrosis in CCl4 -treated mice does not increase.

A. Representative example of FACS contour plots displays gating strategy used to identify $CD8^+$ T cell population. First gated on lymphocytes by FSC-A and SSC-A; singlets by FSC-H and FSC-A, viability by using live/dead marker, then excluding B lymphocytes by using CD19 marker to define positive CD8 T cells. Top panel shows control sample (blue), bottom panel shows CCl4-treated mouse sample (red). **B.** Representative figure of gating strategy to assess the expression of $CD107^+$ $CD8^+$ T, using the unstimulated sample. C. Peripheral blood mononuclear cells (PBMCs) were stimulated with anti-CD3/CD28 (5mg/mL)/ (2ug/mL) antibodies for 48 hours, then labeled with functional antibodies for $CD107a^+$ $CD8^+$ T cells. The proportion (%) of $CD107a^+$ $CD8^+$ T cells in controls and CCl_4-treated mice. **C.** Study C; **D.** Study B. Results from control and CCl_4-treated mice are shown in blue and red, respectively. Data are presented as means ($\pm$SD), statistical significance between the two groups was determined using a two-tailed unpaired Students' *t*-test to compare CCl_4-treated mice vs. controls (*$p<0.05$).

Expression of the cytolytic molecule granzyme B (GrzB) was assessed in bulk $CD8^+$ T cells in the control and CCl_4-treated mice. After stimulating PBMC *in vitro*, GrzB expression was significantly induced by anti-CD3/28 in both treated groups across all experiments compared to unstimulated samples. In Exp A, however, unlike CD107a expression, the proportion of $GrzB^+$ $CD8^+$ T cells was significantly higher ($p > 0.05$) in CCl_4-treated mice compared to the controls at the peak of liver fibrosis (Fig. 5B). This hyperfunction of $GrzB^+$ $CD8^+$ T cells was detected again in study C in the CCl_4-treated mice, which developed advanced liver fibrosis scored with ≥F3 (Fig. 5C). When we looked to $CD8^+$ T cell subpopulation, we found all CD8 T cell subsets (naïve, effector, central memory) were contributing in observed hyperfunction of GrzB in CCl_4-treated mice compared to the controls (Fig. 5E). These results were observed consistently across all six independent experiments in both sexes of CCl_4-treated mice, suggesting that advanced liver fibrosis is associated with $GrzB^+$ $CD8^+$ T cell induction with all subsets contributing to this hyperfunctionality. While % $CD107a^+$ $CD8^+$ T cells did not reflect the hyperfunction mediated by liver fibrosis, the proportion of $GrzB^+CD107a^+$ cells in bulk $CD8^+$ T cells was three times higher in fibrotic mice than the controls at week 12, with over 50% of $GrzB^+$ $CD8^+$ T cells co-expressing $CD107a^+$(Fig. 5F).

A)

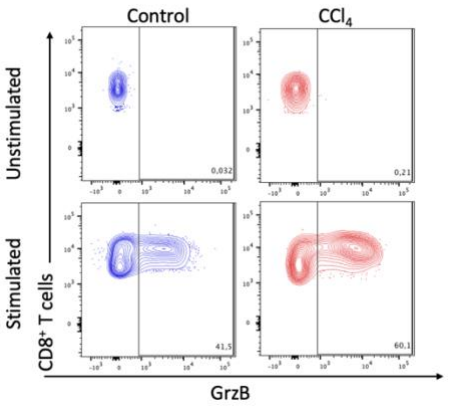
Control
CCl4
Unstimulated
Stimulated
CD8+ T cells
GrzB

B)

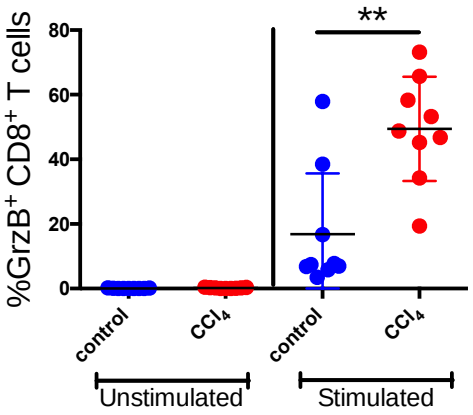
%GrzB+ CD8+ T cells
**
control
CCl4
control
CCl4
Unstimulated
Stimulated

C)

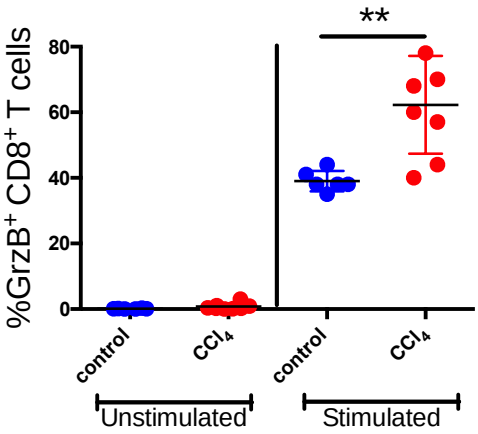
%GrzB+ CD8+ T cells
**
control
CCl4
control
CCl4
Unstimulated
Stimulated

D)

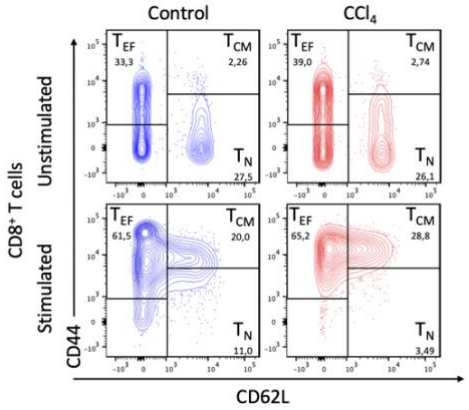
Control
CCl4
CD8+ T cells
Unstimulated
Stimulated
CD44
CD62L
TEF
TCM
TN

E)

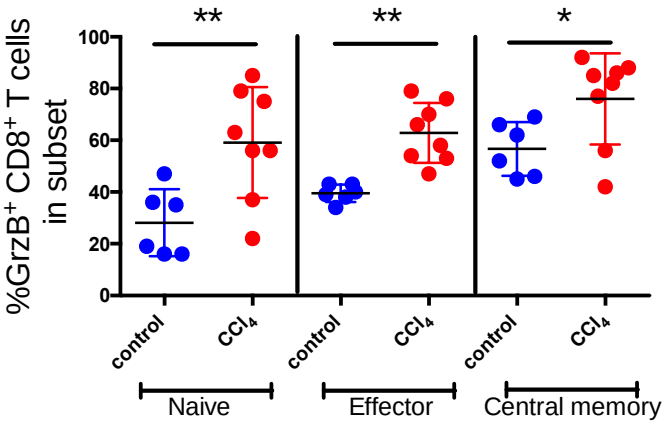
%GrzB+ CD8+ T cells in subset
**
**
*
control
CCl4
control
CCl4
control
CCl4
Naive
Effector
Central memory

F)

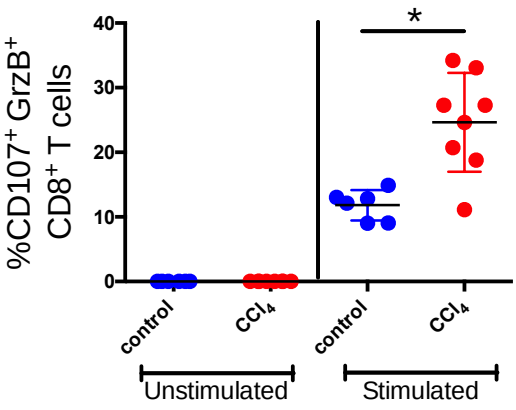
%CD107+ GrzB+ CD8+ T cells
*
control
CCl4
control
CCl4
Unstimulated
Stimulated

Figure 5. **Increased proportion of Granzyme B in advanced liver fibrosis in CCl4 -induced at week12.**

A. Representative FACS contour plots of gating strategy to assess the expression of GrzB $^{+}$ $CD8^{+}$ T cells, using the unstimulated sample. PBMCs were stimulated with anti-CD3/CD28 antibodies for 48 hours, then labeled with functional antibodies $GrzB^{+}$ $CD8^{+}$ T cells and assessed by flow cytometry on bulk $CD8^{+}$ T cells. **B.** Study B, **C.** Study C, the proportion of $GrzB^{+}$ $CD8^{+}$ T cells in CCl_4-treated mice (in red) and control mice (in blue). **D.** Gating strategy for $CD8^{+}$ T cell subpopulation using the surface markers CD62L and CD44 to distinguish $CD8^{+}$ T cell subsets as following as: naïve ($CD44^{low}$, $CD62L^{+}$), effector ($CD44^{+}$, $CD62L^{-}$), and memory ($CD44^{+}$, $CD62L^{+}$). **E.** GrzB expression on $CD8^{+}$ T cell subset in CCl_4-treated mice compared to controls. **F.** Increased proportion of bi-functional CD107a + $GrzB^{+}$ $CD8^{+}$ T cells in CCl_4-treated mice with advanced liver fibrosis (in red) and control mice (in blue) (study C). Data are presented as ($\pm$SD), statistical analysis determined using (*$p<0.05$, or **$p<0.001$) a two-tailed unpaired Students' *t*-test to compare CCl_4-treated mice vs. controls.

3.2.b. $CD8^+$ T cell cytokine expression in advanced liver fibrosis

The induction of the immunomodulatory interferon-γ (IFN-γ) cytokine was also measured at the peak of liver fibrosis (≈week 12) on bulk $CD8^+$ T cells. The proportion of IFN-γ^+ cells significantly increased in both groups after *in vitro* stimulation with anti-CD3/28 compared to unstimulated cells. In study B, the percentage of IFN-γ^+ $CD8^+$ T cells was significantly elevated in CCl_4-treated mice, all of whom scored ≥F3 compared to control oil mice (p>0,05, Fig. 6B). In study C, there was a trend (p=0.06) towards an elevated proportion of IFN-γ^+ $CD8^+$ T cells in CCl_4-treated mice with advanced liver fibrosis compared to the controls. This high expression of IFN-γ^+ on circulating $CD8^+$ T was also seen in other studies that were conducted for this project with effector $CD8^+$ T cells being the most contributing subset in this hyperfunctionality (Fig. 6D). These data show that $CD8^+$ T cell hyperfunctionality is associated with liver fibrosis severity in this mouse model, confirming findings in HCV-infected humans wherein $CD8^+$ T hyperfunction was described as an increased percentage of IFN-γ^+ $CD8^+$ T cells with advanced liver fibrosis, particularly effector CD8+ T cells[111]. We also found an elevated proportion of IFN-γ^+ $CD8^+$ T cells co-expressing CD107a and GrzB in fibrotic mice, with a proportion twice what was observed in the controls, demonstrating their pronounced poly function (Fig. 6D). No sex effect was observed in the assessment of IFN-γ^+ expression.

A)

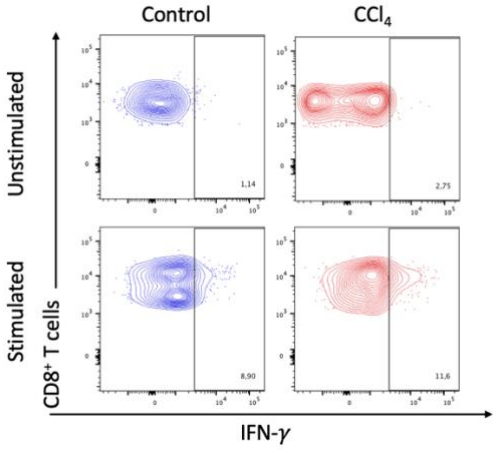
Control
CCl4
Unstimulated
Stimulated
CD8+ T cells
IFN-γ

B)

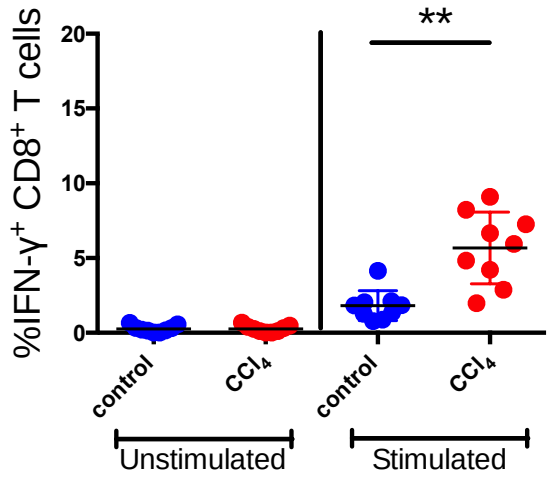
%IFN-γ+ CD8+ T cells
**
control
CCl4
control
CCl4
Unstimulated
Stimulated

C)

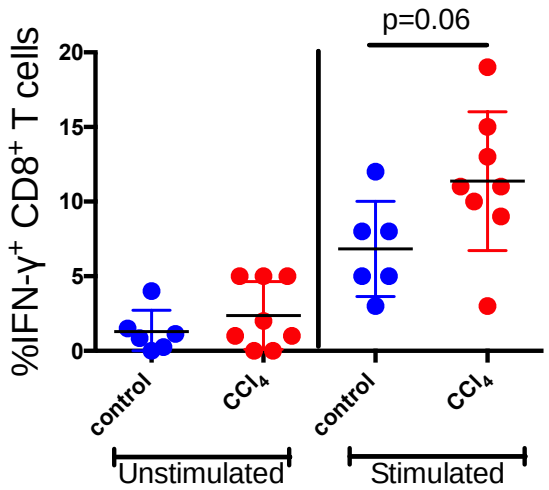
%IFN-γ+ CD8+ T cells
p=0.06
control
CCl4
control
CCl4
Unstimulated
Stimulated

D)

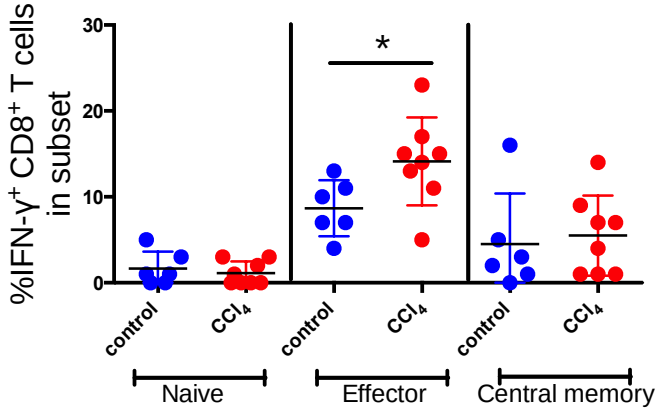
%IFN-γ+ CD8+ T cells in subset
*
control
CCl4
control
CCl4
control
CCl4
Naive
Effector
Central memory

E)

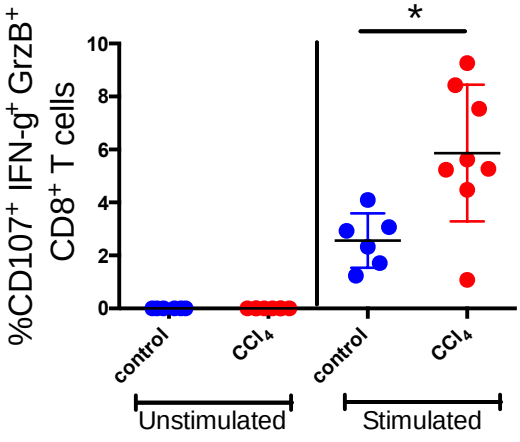
%CD107+ IFN-g+ GrzB+ CD8+ T cells
*
control
CCl4
control
CCl4
Unstimulated
Stimulated

Figure 6. Increased proportion of IFN-γ^+ CD8$^+$ T cells in advanced liver fibrosis in CCl4-model.

A. Representative FACS contour plots of gating strategy to assess the expression of IFN-γ^+ CD8$^+$ T cells, using the unstimulated sample. PBMCs were stimulated with anti-CD3/CD28 antibodies for 48 hours, then labeled with functional antibodies IFN-γ^+ CD8$^+$ T cells and assessed by flow cytometry on bulk CD8$^+$ T cells. **B.** Study B, **C.** Study C, the percentage of IFN-γ^+ CD8$^+$ T cells in CCl_4-treated mice (in red), and control mice (in blue). **D.** IFN-γ^+ expression on CD8$^+$ T cell subsets in CCl_4-treated mice compared to controls. **E.** Increased oligo-functional CD8$^+$ T cells (CD107a$^+$ + IFN-γ^+ + GrzB$^+$) in advanced liver fibrosis. Data are presented as ($\pm$SD), statistical analysis determined using (*p<0.05, or **p<0.001) a two-tailed unpaired Students' *t*-test to compare CCl_4-treated mice vs. controls. Where relevant, statistical trends are indicated (p<0.07).

The proinflammatory cytokine, tumor necrosis factor-α (TNF-α) in bulk $CD8^+$ T cells was assessed at the peak of liver fibrosis severity. In response to anti-CD3/28 stimulation *in vitro*, the proportion of TNF-α^+ cells increased significantly in both groups. In study B, we noticed a significant reduction in the proportion of TNF-α^+ bulk $CD8^+$ T cells in CCl_4-treated mice compared to oil controls at the peak of liver fibrosis ($p>0.0006$), and this contrasted to the IFN-γ data, in the same experiment. However**,** in experiment C, no alterations were observed in the expression of TNF-α on circulating $CD8^+$ T cells between CCl_4-treated mice or controls after 12 weeks of treatment. These inconsistent data, perhaps due to technical reasons related to flow cytometry, make it difficult to draw a definitive conclusion as to whether there is an association between TNF-α production and advanced liver fibrosis (Fig. 7).

A)

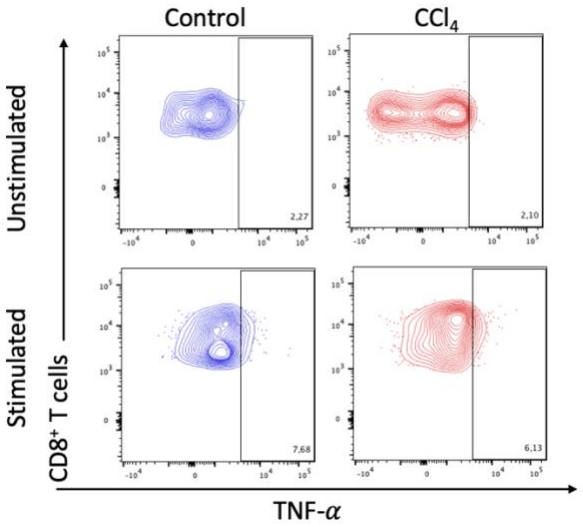
Control
CCl4
Unstimulated
Stimulated
CD8+ T cells
TNF-α
2,27
2,10
7,68
6,13

B)

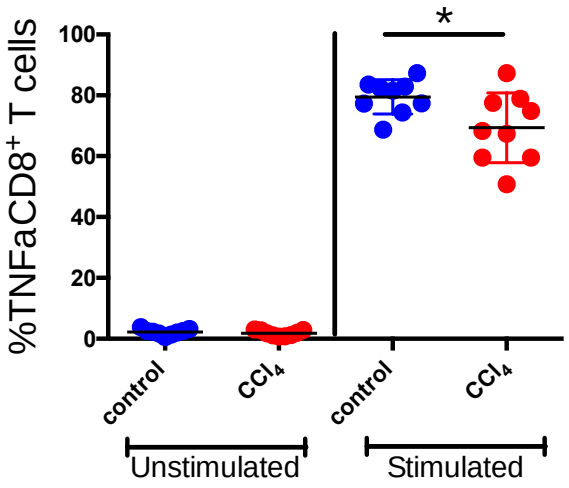
%TNFaCD8+ T cells
100
80
60
40
20
0
*
control
CCl4
control
CCl4
Unstimulated
Stimulated

C)

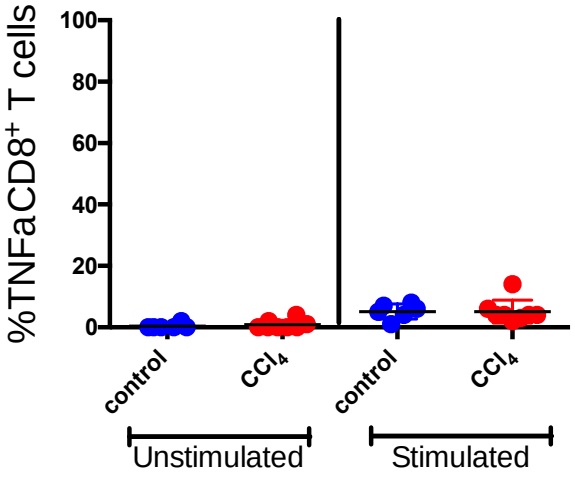
%TNFaCD8+ T cells
100
80
60
40
20
0
control
CCl4
control
CCl4
Unstimulated
Stimulated

Figure 7. No change in TNF-α+ CD8+ T cells in advanced liver fibrosis in CCl4 model.

A. Representative FACS contour plots of gating strategy to assess the expression of TNF-α^+ $CD8^+$ T cells, using the unstimulated sample. PBMCs were stimulated with anti-CD3/CD28 antibodies for 48 hours, then labeled with functional antibodies TNF-α^+ $CD8^+$ T cells and assessed by flow cytometry on bulk $CD8^+$ T cells. **B.** Study B. **C.** study C, the percentage of TNF-α^+ $CD8^+$ T cells in CCl_4-treated mice (in red), and control mice (in blue). PBMCs were stimulated with anti-CD3/CD28 antibodies for 48 hours, then labeled with functional antibodies for TNF-α^+ $CD8^+$ T cells. Data are presented as ($\pm$SD), statistical analysis determined using (*$p<0.05$, or **$p<0.001$) a two-tailed unpaired Students' *t*-test to compare CCl_4-treated mice vs. controls.

3.2.c. Induction of CD8+ T cell activation markers expression in advanced liver fibrosis in CCl4 model.

In this model of liver fibrosis, we also investigated PD-1 expression, an inhibitory molecule expressed early after activation on $CD8^+$ T cells. First, the baseline level of PD-1 expression did not differ between the study groups. At week 12, in study B, we did not observe any change in the induction of PD-1 expression on bulk $CD8^+$ T cells with significantly elevated levels in fibrotic mice compared to the controls ($p=0.02$). In experiment B, both groups of mice increased PD-1 expression following stimulation, but there were no significant differences between groups ($p=0.08$) (Fig. 8B). This shows $CD8^+$ T cells are equivalently activated in advanced liver fibrosis.

A)

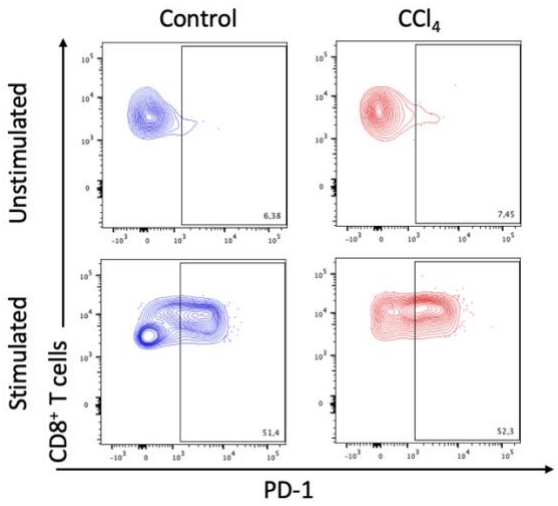
Control
CCl4
Unstimulated
Stimulated
CD8+ T cells
PD-1
6,38
7,45
51,4
52,3

B)

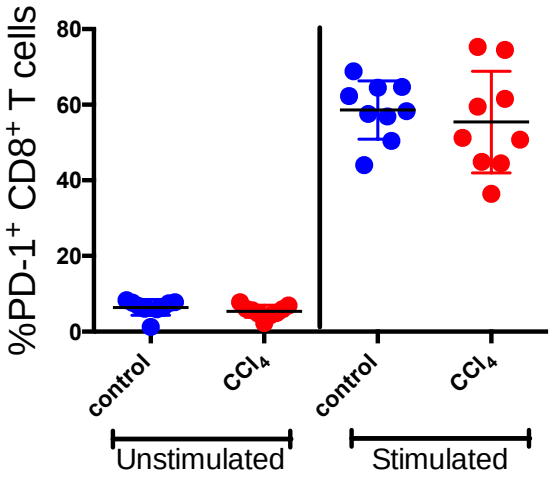
%PD-1+ CD8+ T cells
80
60
40
20
0
control
CCl4
control
CCl4
Unstimulated
Stimulated

Figure 8. No change in the expression of PD-1 CD8+ T cells in advanced liver fibrosis in mice.

Representative FACS contour plots of gating strategy to assess the expression of PD-1^+ $CD8^+$ T cells, using the unstimulated sample. PBMCs were stimulated with anti-CD3/CD28 antibodies for 48 hours, then labeled with activation marker PD-1^+ $CD8^+$ T cells and assessed by flow cytometry on bulk $CD8^+$ T cells. **B.** Study B, the percentage of PD-1^+ between CCl_4-treated mice (in red) and control mice (in blue). Data are presented as ($\pm$SD), statistical analysis determined using (*$p<0.05$, or **$p<0.001$) a two-tailed unpaired Students' *t*-test to compare CCl_4-treated mice vs. controls.

The expression of NKG2D, another activation marker and regulatory protein, was assessed in the presence of advanced liver fibrosis. We observed that the induction of NKG2D was significantly lower in mice treated with CCl_4 compared to control mice at the peak of liver fibrosis. These results were unexpected but consistent in three independent studies (A, B, and C), performed in this model of liver fibrosis (Fig. 9A-B). These results indicate that advanced liver fibrosis might have a noticeable impact on this indicator of T cell activation and regulation.

A)

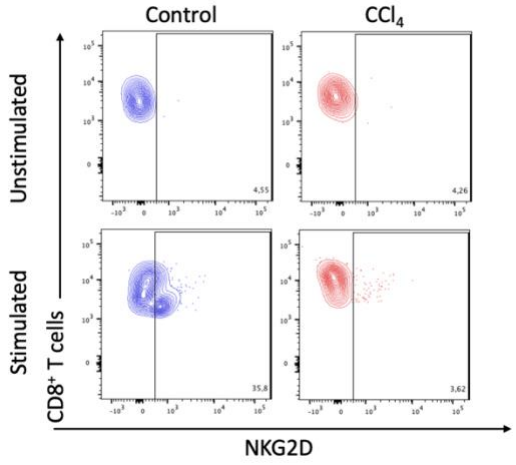
Control
CCl4
Unstimulated
Stimulated
CD8+ T cells
NKG2D

B)

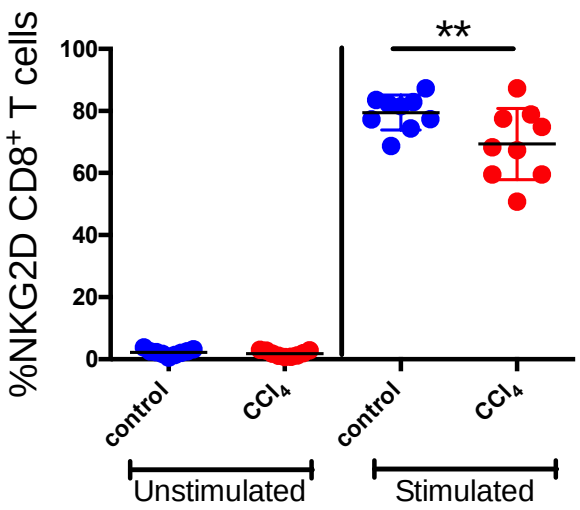
%NKG2D CD8+ T cells
100
80
60
40
20
0
**
control
CCl4
control
CCl4
Unstimulated
Stimulated

C)

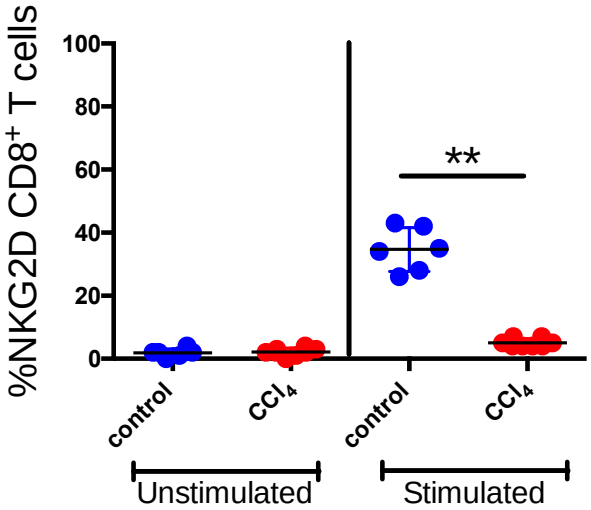
%NKG2D CD8+ T cells
100
80
60
40
20
0
**
control
CCl4
control
CCl4
Unstimulated
Stimulated

Figure 9. NKG2D expression in advanced liver fibrosis model.

A. Representative FACS contour plots of gating strategy to assess the expression of $NKG2D^+$ $CD8^+$ T cells, using the unstimulated sample. PBMCs were stimulated with anti-CD3/CD28 antibodies for 48 hours, then labeled with activation marker $NKG2D^+$ $CD8^+$ T cells and assessed by flow cytometry on bulk $CD8^+$ T cells. **B.** Study B. **C.** Study C. The percentage of $NKG2D^+$ between CCl_4-treated mice (in red) and control mice (in blue). Data are presented as ($\pm$SD), statistical analysis determined using (*$p<0.05$, or **$p<0.001$) a two-tailed unpaired Students' *t*-test to compare CCl_4-treated mice vs. control mice.

3.3. $CD8^+$ T cell hyperfunction with progressive liver fibrosis

3.3.a. Cytolytic molecule expression over time: $CD107a^+$/ $GrzB^+$

It has been documented that early signs of fibrosis can be detected in the mouse liver after two to three weeks of CCl_4 exposure whereas severe scarring and excessive tissue deposition are evident with the continuous toxic treatment after four to six weeks, depending on the dosage, frequency, and route of exposure[55]. In this project we have shown that in this model the fibrosis score of the liver is F1/2 at seven weeks and achieved F3/4 after 12 weeks of treatment with CCl_4 (Fig. 2). To better associate $CD8^+$ T cell hyperfunction with the attainment of advanced liver fibrosis, the initiation and dynamics of $CD8^+$ hyperfunction was assessed over time. To achieve this during the early phases of liver injury (i.e. minimal fibrosis), blood samples were collected at early time points (weeks 0, 4, 8) in four independent experiments (Table 1). After *in vitro* stimulation with anti-CD3/28, the degranulation marker CD107a was detected in controls and CCl_4-treated mice in all four studies (weeks 0, 4,8), yet no statistical significance was observed between the two groups and no sex effects were detected in most of the studies (three out of four). Study C was the only exception a more significant reduction was observed in CCl_4-treated mice than in the controls (Fig. 4D). Over time, there was a transient trending in the induction of $CD107a^+$ $CD8^+$ T cells eight weeks after CCl_4 treatment, but it was not observed earlier or later in liver fibrosis progression (Fig. 10). This indicates that fibrosis progression is not associated with the expression of $CD107a^+$ $CD8^+$ T cells and at the peak of liver fibrosis (week 12), as shown in (Fig. 4A).

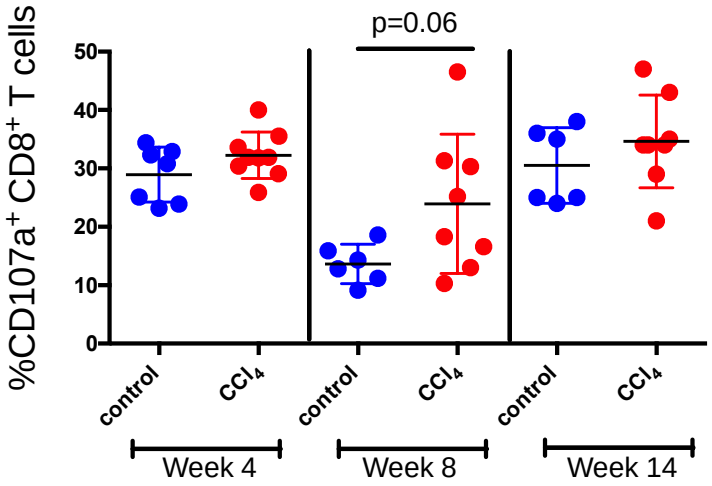
%CD107a+ CD8+ T cells
p=0.06
50
40
30
20
10
0
control
CCl4
control
CCl4
control
CCl4
Week 4
Week 8
Week 14

Figure 10. No change in CD107a+ CD8+ T cells detection in liver fibrosis progression.

Blood was collected from mice at 4-, 8-, and 14-weeks post CCl_4 administration. PBMCs were stimulated with anti-CD3/CD28 antibodies for 48 hours, then labeled with functional markers $CD107a^+$ $CD8^+$ T cells and assessed by flow cytometry on bulk $CD8^+$ T cells. Study C, the proportion of IFN-γ^+ $CD8^+$ T cells in CCl_4-treated mice (in red) and control mice (in blue) (n=18). Data are presented as ($\pm$SD), statistical analysis determined using (*$p<0.05$, or **$p<0.001$) a two-tailed unpaired Students' *t*-test to compare CCl_4-treated mice vs. control mice.

The induction of $GrzB^+$ was measured at early time points (weeks 0, 4, 8) in liver fibrosis progression. *In vitro* stimulation with anti-CD3/28 significantly induced the expression of $GrzB^+$ in both study groups, although the timing when this occurred in the CCl_4 protocol (i.e. weeks 4 or 8) was variable across studies. In experiment C, the proportion of $GrzB^+$ cells in bulk $CD8^+$ T cells was significantly greater in CCl_4-treated mice than controls in both sexes, after four weeks of the treatment ($p>0.03$). This difference was two fold higher in treated mice than the controls at the peak of liver fibrosis at week 14 ($p>0.002$) (Fig. 11). Overall, these data show that progressive liver fibrosis occurs alongside a mounting hyperfunction of $CD8^+$ T cells marked by $GrzB^+$ expression. This significant increase in $GrzB^+$ $CD8^+$ T cells in CCl_4-treated mice at earlier time points of receiving the liver insult suggests a strong association between $GrzB^+$ up-regulation and liver fibrosis severity.

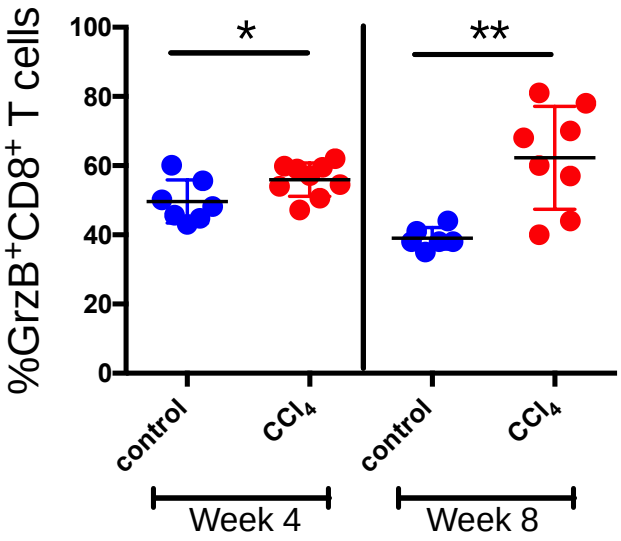
%GrzB+CD8+ T cells
100
80
60
40
20
0
*
**
control
CCl4
control
CCl4
Week 4
Week 8

Figure 11. Increased GrzB+ CD8+ T cells expression in liver fibrosis progression.

Blood was collected from mice at 4-, and 14-weeks post CCl_4 administration. PBMCs were stimulated with anti-CD3/CD28 antibodies for 48 hours, then labeled with functional markers $GrzB^+$ $CD8^+$ T cells and assessed by flow cytometry on bulk $CD8^+$ T cells. Study C, the proportion of IFN-γ^+ $CD8^+$ T cells in CCl_4-treated mice (in red) and control mice (in blue) (n=18). Data are presented as ($\pm$SD), statistical analysis determined using (*$p<0.05$, or **$p<0.001$) a two-tailed unpaired Students' *t*-test to compare CCl_4-treated mice vs. control mice.

3.3.b. Cytokine expression: IFN- γ/TNFα

Following in vitro stimulation and intercellular staining, no change was observed in the proportion of IFN-γ^+ bulk $CD8^+$ cells in response to stimulation between CCl_4-treated mice and control mice. In early stages of liver fibrosis, weeks 0, 4, 8, all four independent experiments displayed an increasing trend of IFN-γ expression in Study C (p=0.06, Fig. 12). However, at the peak of liver fibrosis (week12/14), a significant elevation was observed in the percentage of IFN-γ^+CD8^+ in fibrotic mice than in the controls (Fig. 6 A-B). These findings indicate that while the proportion of IFN-γ $CD8^+$ cells was elevated at the peak of fibrosis, this was not observed through the period of fibrosis progression.

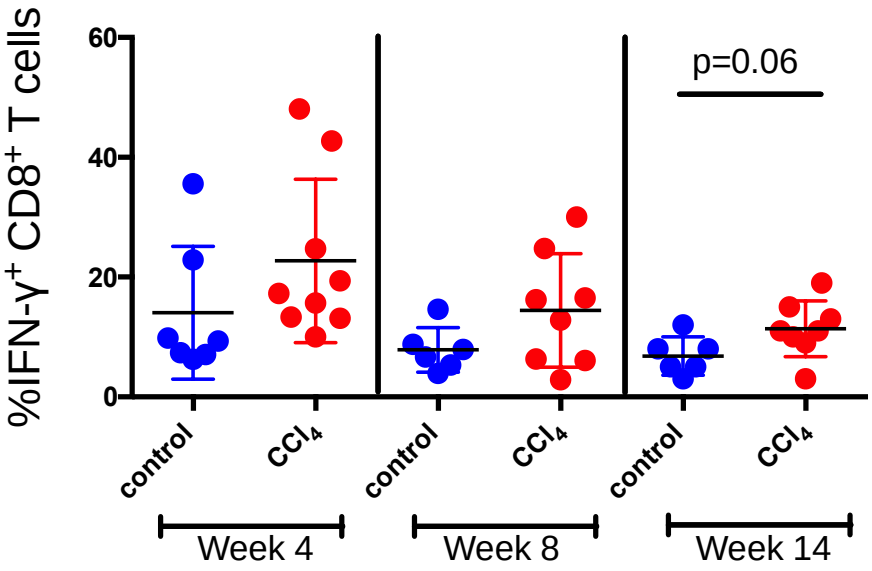
%IFN-γ+ CD8+ T cells
60
40
20
0
p=0.06
control
CCl4
control
CCl4
control
CCl4
Week 4
Week 8
Week 14

Figure 12. No change in IFN-γ+ CD8+ T cells expression in liver fibrosis progression.

Blood was collected from mice at 4-, 8- and 14-weeks post CCl_4 administration. PBMCs were stimulated with anti-CD3/CD28 antibodies for 48 hours, then labeled with functional markers IFN-γ^+ $CD8^+$ T cells and assessed by flow cytometry on bulk $CD8^+$ T cells. Study C, the proportion of IFN-γ^+ $CD8^+$ T cells in CCl_4-treated mice (in red) and control mice (in blue) (n=18). Data are presented as ($\pm$SD), statistical analysis determined using (*$p<0.05$, or **$p<0.001$) a two-tailed unpaired Students' *t*-test to compare CCl_4-treated mice vs. control mice.

At the peak of liver fibrosis, ≈week 12, we noted that there was hyperfunction defined by the expression of $GrzB^+$ and IFN-γ^+ but not in TNF-α expression (Fig. 7). Therefore, the proportion of the immunomodulatory cytokine TNF-α on $CD8^+$ T cells between CCl_4-treated mice and the controls was also assessed during liver fibrosis progression (weeks 0, 4, 8) in four independent experiments. After anti-CD3/28 stimulation, no change in the expression of TNF-α^+ on bulk $CD8^+$ T cells was seen at earlier time points (weeks 4 and 8) in three out of four experiments. In experiment C, however, the proportion of TNF-α^+ $CD8^+$ T cells significantly increased in CCl_4-treated mice at early fibrosis (week 4), and significantly decreased in experiment D at week 9 only. These inconsistent results between the two groups were not observed later at the peak of liver fibrosis, suggesting this change might be transient (Fig. 13). This is confirmed given the overall lack of elevated TNF-α^+ cells at the peak of fibrosis in several studies (Fig. 7).

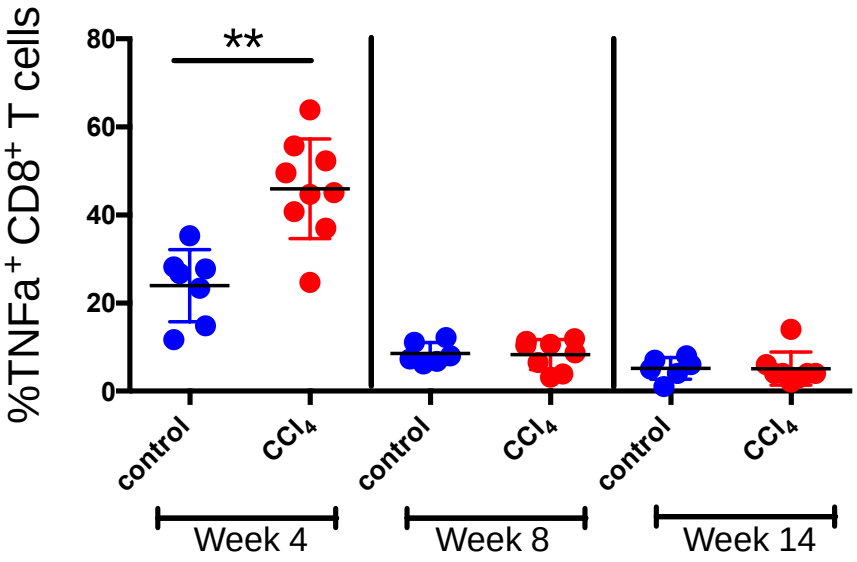
%TNFa+ CD8+ T cells
80
60
40
20
0
**
control
CCl4
control
CCl4
control
CCl4
Week 4
Week 8
Week 14

Figure 13. No change in TNF-α+ CD8+ T cells expression in liver fibrosis progression.

Blood was collected from mice at 4-, 8- and 14-weeks post CCl_4 administration. PBMCs were stimulated with anti-CD3/CD28 antibodies for 48 hours, then labeled with functional markers TNF-α^+ $CD8^+$ T cells and assessed by flow cytometry on bulk $CD8^+$ T cells. Study C, the proportion of TNF-α^+ $CD8^+$ T cells in CCl_4-treated mice (in red) and control mice (in blue) (n=18). Data are presented as ($\pm$SD), statistical analysis determined using (*$p<0.05$, or **$p<0.001$) a two-tailed unpaired Students' *t*-test to compare CCl_4-treated mice vs. control mice.

3.3.c. Activation markers: PD-1/NKG2D

PD-1 expression on $CD8^+$ T cells was measured during liver fibrosis progression (weeks 4, 8). There was no difference in the proportion of $PD\text{-}1^+$ $CD8^+$ T cells between CCl_4 treated-mice compared to controls at weeks 4 and 8 in four independent experiments. The only exception was week 4 in study C when there was a significant general increase in the percentage of $PD\text{-}1^+$ $CD8^+$ T cells in CCl_4 treated-mice as opposed to the controls ($p>0.03$) before this gap between the two groups almost disappeared to control levels in later weeks of treatment (Fig. 14). This suggests this significant expression was transient, and it might not be associated with the severity of liver fibrosis.

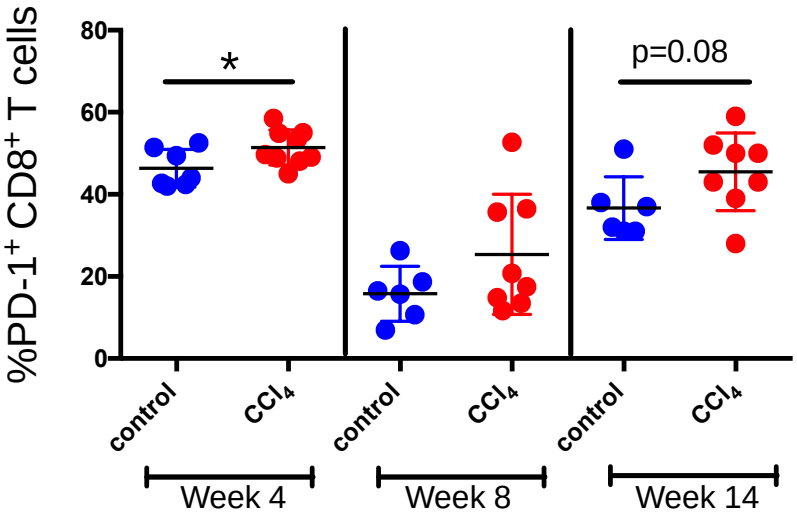
%PD-1+ CD8+ T cells
80
60
40
20
0
*
p=0.08
control
CCl4
control
CCl4
control
CCl4
Week 4
Week 8
Week 14

Figure 14. No change in PD-1$^+$ CD8$^+$ T cells expression in fibrosis progression.

Blood was collected from mice at 4, 8 and 14 weeks post CCl_4 administration. PBMCs were stimulated with anti-CD3/CD28 antibodies for 48 hours, then labeled with functional markers PD-1$^+$ CD8$^+$ T cells and assessed by flow cytometry on bulk CD8$^+$ T cells. Study C, the proportion of PD-1$^+$ CD8$^+$ T cells in CCl_4-treated mice (in red) and control mice (in blue) (n=18). Data are presented as ($\pm$SD), statistical analysis determined using (*$p<0.05$, or **$p<0.001$) a two-tailed unpaired Students' *t*-test to compare CCl_4-treated mice vs. control mice.

After 12 weeks of the treatment with CCl_4, expression of the activation marker NKG2D was significantly lower in CCl_4-treated mice compared to controls upon *in vitro* stimulation with anti-CD3/28 in multiple studies (Fig. 9). Therefore, we measured the proportion of $NKG2D^+$ $CD8^+$ T cells during liver fibrosis progression (weeks 0, 4, 8). No changes were observed in the percentage of NKG2D between CCl_4-treated mice and controls during liver fibrosis progression (i.e. weeks 4, 8) whereas at the peak of liver fibrosis, there was a statistical significance between the two groups marked by a significance reduction in CCl_4-treated mice compared to the controls (Fig. 15). This implies an association between the severity of liver fibrosis and bulk $CD8^+$ T cell activation, particularly NKG2D, alongside hyperfunction (e.g. IFN-γ and GrzB).

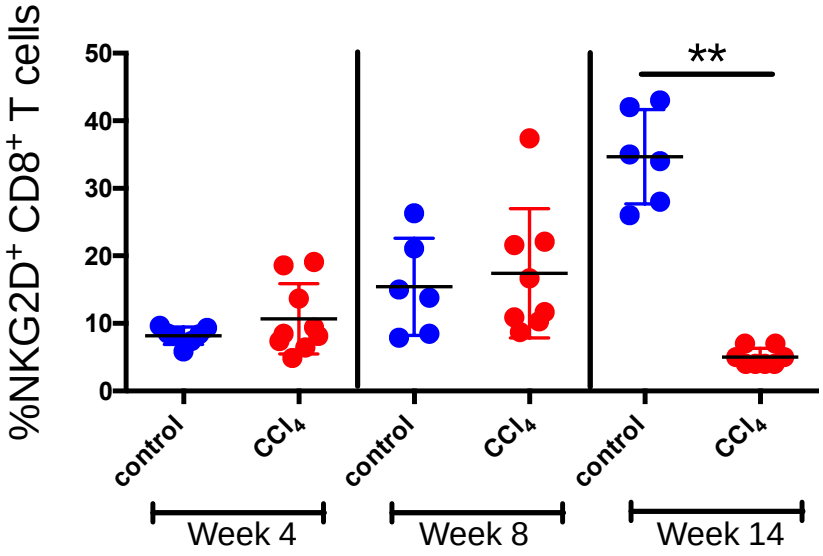
%NKG2D+ CD8+ T cells
50
40
30
20
10
0
**
control
CCl4
control
CCl4
control
CCl4
Week 4
Week 8
Week 14

Figure 15. Lower NKG2D+ CD8+ T cells expression in liver fibrosis progression.

Blood was collected from mice at 4-, 8- and 14-weeks post CCl_4 administration. PBMCs were stimulated with anti-CD3/CD28 antibodies for 48 hours, then labeled with functional markers $NKG2D^+$ $CD8^+$ T cells and assessed by flow cytometry on bulk $CD8^+$ T cells. Study C, the proportion of $NKG2D^+CD8^+$ T cells in CCl_4-treated mice (in red) and control mice (in blue) (n=18). Data are presented as ($\pm$SD), statistical analysis determined using (*$p<0.05$, or **$p<0.001$) a two-tailed unpaired Students' *t*-test to compare CCl4-treated mice vs. control mice.

3.4. $CD8^+$ T cell function following liver fibrosis regression

3.4.a. Cytolytic molecules induction in advanced liver fibrosis: 4-7 weeks post CCl_4 cessation

In this project we report that liver fibrosis in the CCl_4 model can regress within 4 weeks following the removal of the liver insult. Therefore, we sought to determine whether $CD8^+$ T cell hyperfunction was sustained following fibrosis regression. This was addressed in experiment E. After inducing advanced fibrosis in mice, treatment was discontinued in some mice at week 16, and $CD8^+$ T cell function was assessed after 4 and 7 weeks. Four weeks post-CCl_4 cessation, following *in vitro* stimulation, no statistical significance was observed in the proportion of $CD107a^+$ bulk $CD8^+$ T cells among with or without continuation or in controls. However, it was significantly detectable on bulk $CD8^+$ T cells in female mice with the ongoing treatment of CCl_4 p= 0.04. Seven weeks post-CCl_4 cessation, significant changes were observed in the detection of $CD107a^+$ on peripheral $CD8^+$ T cells in fibrotic mice with or without CCl_4 continuation compared to controls in both sexes. These results of maintained elevation of the degranulation $CD107a^+$ on circulating $CD8^+$ T cells were seen in HCV^+ individuals with advanced liver fibrosis (F3/4) compared to minimal fibrosis (F1/2) long after SVR, showing the long term of chronic liver diseases and advanced liver fibrosis are associated with hyperfunction of $CD107a^+$ on bulk $CD8^+$ cells regardless of liver etiology.

A)

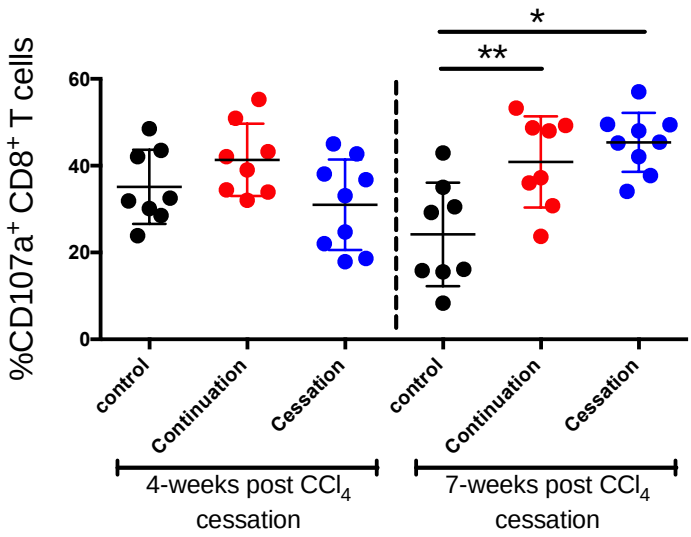
%CD107a+ CD8+ T cells
60
40
20
0
*
**
control
Continuation
Cessation
control
Continuation
Cessation
4-weeks post CCl4 cessation
7-weeks post CCl4 cessation

B)

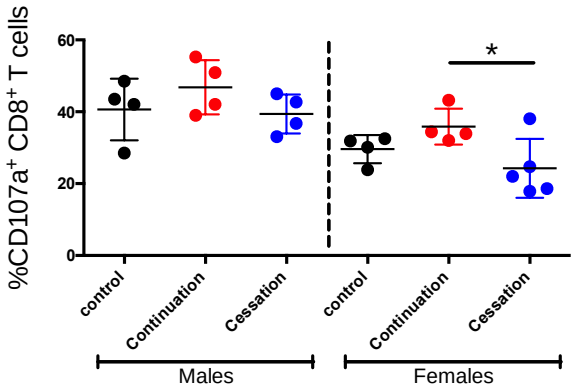
%CD107a+ CD8+ T cells
60
40
20
0
*
control
Continuation
Cessation
control
Continuation
Cessation
Males
Females

C)

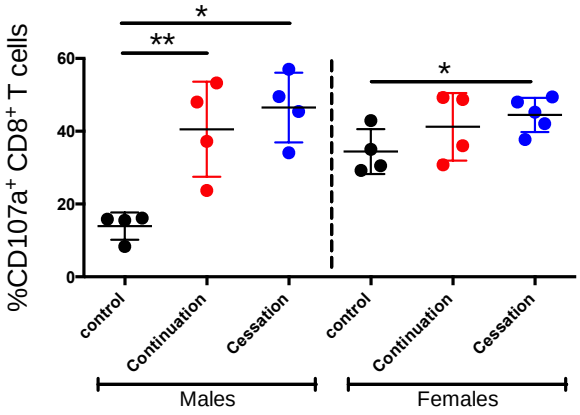
%CD107a+ CD8+ T cells
60
40
20
0
*
**
*
control
Continuation
Cessation
control
Continuation
Cessation
Males
Females

Figure 16. Hyperfunctional CD107a+ CD8+ T cells with liver fibrosis regression.

$CD8^+$ T cell functions were assessed at weeks19 and 21 after some mice stopped receiving the liver insult (CCl_4). **A.** 4 and 7-weeks post-cessation, **B.** Sex effect (4 weeks post-cessation) **C.** Sex effect (7 weeks post-cessation). Isolated PBMCs were stimulated anti-CD3/CD28 antibodies for 48 hours, then labeled with the functional marker of $CD107a^+$ $CD8^+$ T cells and assessed by flow cytometry. The proportion of $CD107a^+$ $CD8^+$ T cells in control (in black), stopped-CCl_4 mice (in blue), and continued-CCl_4 mice (in red). Data are presented as ($\pm$SD), statistical analysis determined using (*$p<0.05$, or **$p<0.001$) a two-tailed unpaired Students' *t*-test to compare CCl4-treated mice vs. control mice.

Four weeks post-CCl_4 cessation after *in vitro* stimulation, induction of $GrzB^+$ in $CD8^+$ T cells was higher in mice treated with CCl_4- treatment, regardless of treatment cessation, compared to controls in both sexes. However, there was no significant difference between the mice that were continuously treated with CCl_4 and those in which treatment was stopped, which might be due to the high degree of individual variation (Fig. 17A). When the data was divided based on sex, there was a clear sex effect in terms of $GrzB^+$ production on bulk $CD8^+$ T cells. There was a general trend towards increased $GrzB^+$ $CD8^+$ T cells in males and the expression of $GrzB^+$ on circulating $CD8^+$ T cells was trending in mice with continuous CCl_4 treatment than in the controls ($p=0.07$). $GrzB^+$ expression was also towards increasing in continuously CCl_4-treated compared to the stopped-CCl_4-treated male mice, while there was no difference between the mice with stopped-CCl_4 treatment and the control male mice (Fig. 17B). In females, on the other hand, there was a dramatic increase in the expression of $GrzB^+$ $CD8^+$ T cells in mice with continuous CCl_4 treatment compared to the controls ($p> 0.001$). For the mice with stopped-CCl_4 treatment, however, there was a significant reduction compared to the controls and mice with continuous-CCl_4 treatment four weeks post-CCl_4 cessation ($p> 0.001$, and 0.001 respectively) (Fig. 17B). This elevated production of $GrzB^+$ was not detected and returned to control levels seven weeks post-CCl_4 cessation and continuation (Fig. 17A, C). This indicates that chronic liver insults (up to 19 weeks of treatment) can result in the sustained tendency to over express $GrzB^+$ on stimulated $CD8^+$ T cells in the circulation with ongoing liver insult and significantly less with the removal of the liver insult , and this effect is more evident in female mice.

A)

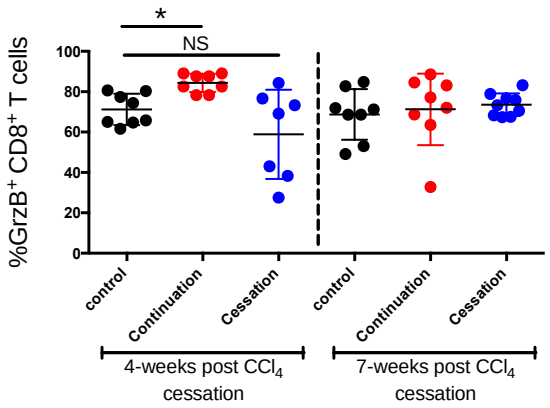
*
NS
%GrzB+ CD8+ T cells
100
80
60
40
20
0
control
Continuation
Cessation
control
Continuation
Cessation
4-weeks post CCl4 cessation
7-weeks post CCl4 cessation

B)

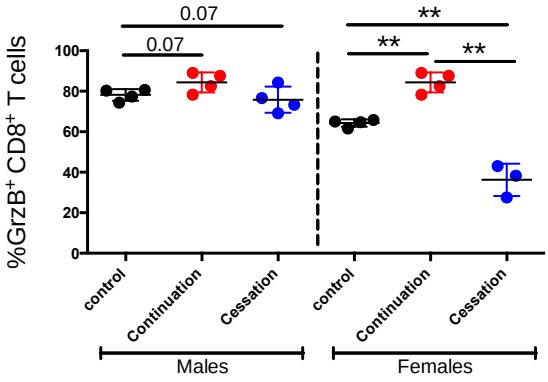
0.07
0.07
**
**
**
%GrzB+ CD8+ T cells
100
80
60
40
20
0
control
Continuation
Cessation
control
Continuation
Cessation
Males
Females

C)

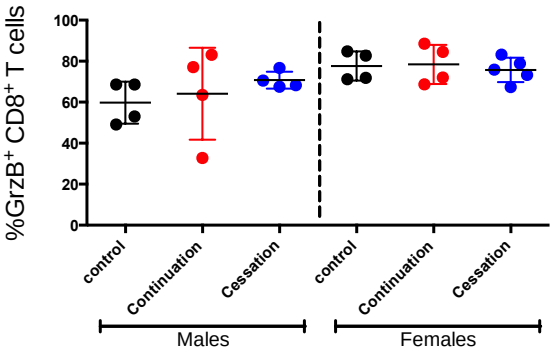
%GrzB+ CD8+ T cells
100
80
60
40
20
0
control
Continuation
Cessation
control
Continuation
Cessation
Males
Females

Figure 17. Sustained GrzB+ hyperfunction in bulk CD8+ T cells after liver fibrosis regression.

$CD8^+$ T cell functions were assessed at weeks 19 and 21 after some mice stopped receiving the liver insult (CCl_4). **A.** 4 and 7-weeks post-cessation, **B.** Sex effect (4 weeks post-cessation) **C.** Sex effect (7 weeks post-cessation). Isolated PBMCs were stimulated anti-CD3/CD28 antibodies for 48 hours, then labeled with the functional marker of $GrzB^+$ $CD8^+$ T cells and assessed by flow cytometry. The proportion of $GrzB^+$ $CD8^+$ T cells in control (in black), stopped-CCl_4 mice (in blue), and continued-CCl_4 mice (in red). Data are presented as ($\pm$SD), statistical analysis determined using (*$p<0.05$, or **$p<0.001$) a two-tailed unpaired Students' *t*-test to compare CCl4-treated mice vs. control mice.

3.4.a. Cytokine expression in advanced liver fibrosis: 4-7 weeks post CCl_4-cessation

After observing $CD8^+$ T cell hyperfunction in the expression of IFN-γ^+ in response to anti-CD3/28 stimulation, we assessed its expression four and seven weeks post-CCl_4 cessation. The proportion of IFN-γ^+ $CD8^+$ T cells significantly increased after *in vitro* stimulation. However, four weeks post-CCl_4 cessation, there was no statistical significance in the expression of IFN-γ on bulk $CD8^+$ T cells among the three study groups (controls, CCl_4- stopped, and continued) in both sexes (Fig. 18 A, B). This is unexpected as we had the best of intentions that the liver would regress, and we still did not see the hyperfunction that was observed multiple times at the peak of liver fibrosis (week 12-14) (Fig. 6). However, seven weeks post-CCl_4 cessation, the proportion of IFN-γ^+ $CD8^+$ T cells were not statistically different in the continuous-CCl_4 fibrotic mice compared to both the CCl_4-cessation mice and the controls. Meanwhile CCl_4-cessation resulted in significantly more IFN-γ^+ $CD8^+$ T cells compared to the controls ($p>0.04$), and it is more outstanding in males (Fig. 18 A, C). This long-lasting hyper-functionality of IFN-γ^+ seven weeks post-CCl_4 is similar to what the lab has shown in HCV-infected individuals with advanced liver fibrosis after treatment, indicating that chronic advanced liver fibrosis has a profound effect on IFN-γ^+ bulk $CD8^+$ T cells even after the removal of the liver insult.

A)

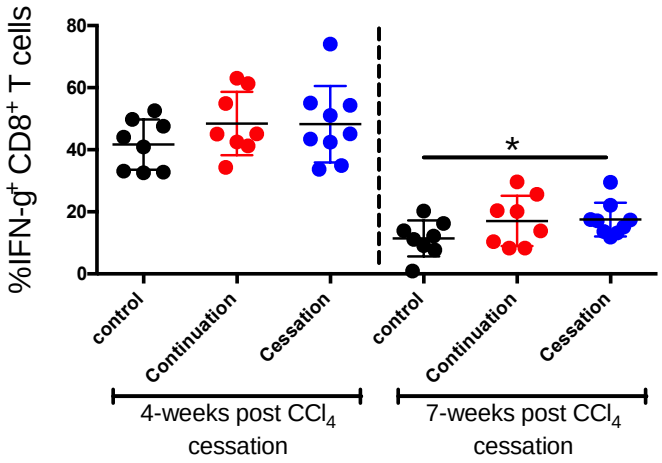
%IFN-g+ CD8+ T cells
80
60
40
20
0
*
control
Continuation
Cessation
control
Continuation
Cessation
4-weeks post CCl4 cessation
7-weeks post CCl4 cessation

B)

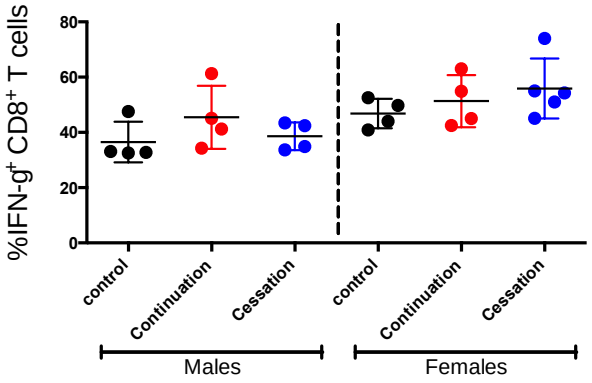
%IFN-g+ CD8+ T cells
80
60
40
20
0
control
Continuation
Cessation
control
Continuation
Cessation
Males
Females

C)

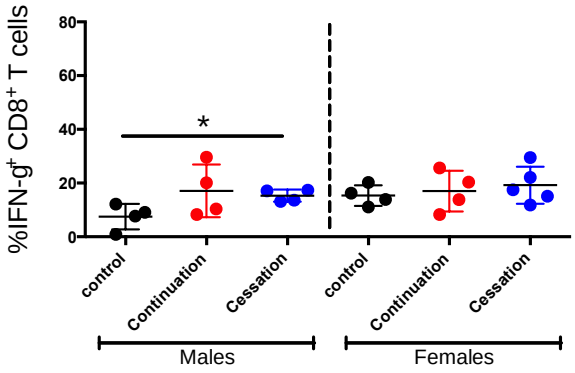
%IFN-g+ CD8+ T cells
80
60
40
20
0
*
control
Continuation
Cessation
control
Continuation
Cessation
Males
Females

Figure 18. Sustained IFN-γ+ hyperfunction in bulk CD8+ T cells after liver fibrosis regression.

$CD8^+$ T cell functions were assessed at weeks 19 and 21 after some mice stopped receiving the liver insult (CCl_4). **A.** 4 and 7-weeks post-cessation, **B.** Sex effect (4 weeks post-cessation) **C.** Sex effect (7 weeks post-cessation). Isolated PBMCs were stimulated anti-CD3/CD28 antibodies for 48 hours, then labeled with the functional marker of IFN-γ^+ $CD8^+$ T cells and assessed by flow cytometry. The proportion of IFN-γ^+ $CD8^+$ T cells in control (in black), stopped-CCl_4 mice (in blue), and continuous-CCl_4 mice (in red). Data are presented as ($\pm$SD), statistical analysis determined using (*p<0.05, or **p<0.001) a two-tailed unpaired Students' *t*-test to compare CCl4-treated mice vs. control mice.

3.5 Immune response in vivo

3.6.a. Tumor growth in advanced liver fibrosis

Individuals with advanced liver fibrosis are at high risk of cancer and negative outcomes, and their specific response are impaired that systemic $CD8^+$ T cell hyperfunction is associated with impaired immunosurveillance. After demonstrating the hyperfunction of $CD8^+$ T cell responses in advanced liver fibrosis, we investigated if this dysfunction reflected a poorer $CD8^+$ T cell response in vivo. MC38 cancer cells were used in this model as they are known to be mediated by robust $CD8^+$ T cell responses[70]. The MC38 cancer cells are derived from grade III adenocarcinoma induced chemically in females C57BL/6 mice [21]; therefore, these studies were conducted exclusively on female mice.

To determine if systemic generalized $CD8^+$ T cell hyperfunction in advanced liver fibrosis affected the response to a tumor challenge, in study B (female mice), once $CD8^+$ T cells hyperfunction was evident at week 12, mice were challenged with a low dose of MC38 tumor cell lines (1×10^5 cells in 100ul PBS) at week 16 and 4 weeks post-CCl_4 continuation. Once palpable, tumor growth was measured every two days until mice reached the endpoint (tumor size: ≈15 mm).

When $CD8^+$ T cell hyperfunction was observed at the peak of liver fibrosis, we also evaluated tumor growth in the context of liver fibrosis progression and regression, so some mice stopped receiving CCl_4 while others kept receiving the hepatotoxic treatment. Four weeks post-CCl_4 cessation, mice were challenged with the same dose of MC38 tumor cells (1×10^5 cells in 100ul PBS). Tumors were detectable after ≈10 days, and the growth in fibrotic mice after CCl_4 cessation was bigger (volume = ≈50 mm^3) compared to the controls (volume = ≈5 mm^3) (Fig.

19B). However, tumor growth was significantly greater in CCl_4-treated mice with continuation compared to the controls ($p<0.05$). This suggests that advanced liver fibrosis and its systemic $CD8^+$ T cell hyperfunction is associated with an impaired response to tumors through an as yet unknown mechanism. This impaired response is sustained somewhat following liver insult removal, yet constant liver insult exacerbates this association.

Mice were also challenged with more cells of the MC38 cancer cell line (3×10^5) at the peak of liver fibrosis (week 12), resulting in similar tumor growth between CCl_4-treated mice and the controls. With a threefold dose, tumors grew within seven days, which was faster than the lower dose. Tumor size was twofold bigger (volume = $\approx$80 mm^3) in all CCl_4-treated mice ($n = 5$) compared to the controls (volume = $\approx$40 mm^3), but with no statistical significance due to the variation within the control group (Fig. 20 D). These data confirm what we have seen in our previous experiments, namely and that advanced liver fibrosis impairs specific immune responses mediated by $CD8^+$ T cells, resulting in rapid tumor growth.

A)

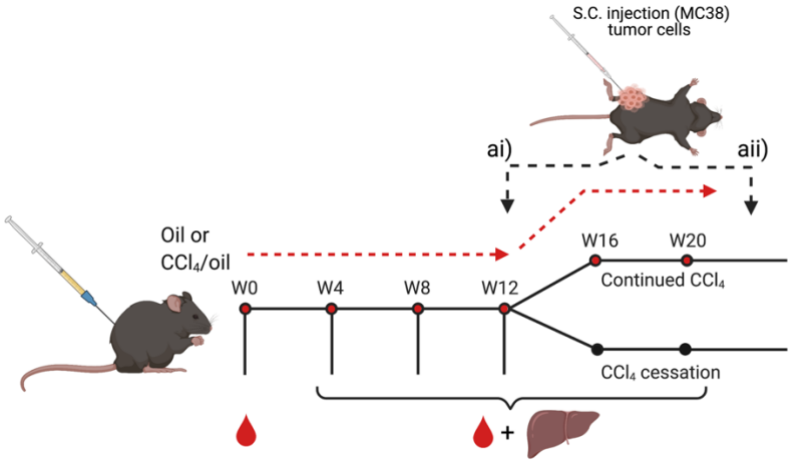
S.C. injection (MC38)
tumor cells
ai)
aii)
Oil or
CCl4/oil
W0
W4
W8
W12
W16
W20
Continued CCl4
CCl4 cessation
+

B)

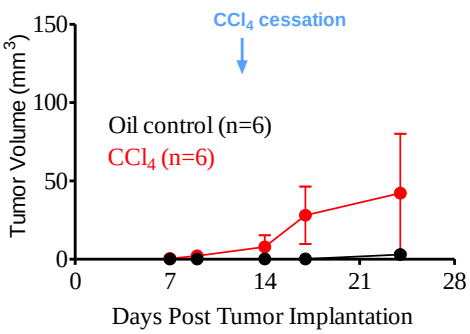
CCl4 cessation
Oil control (n=6)
CCl4 (n=6)
Tumor Volume (mm3)
Days Post Tumor Implantation

C)

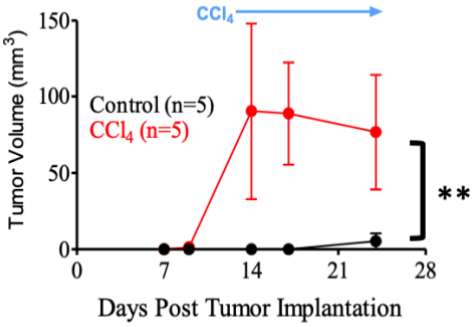
CCl4
Control (n=5)
CCl4 (n=5)
**
Tumor Volume (mm3)
Days Post Tumor Implantation

D)

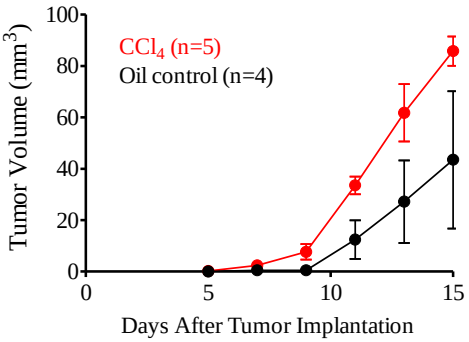
CCl4 (n=5)
Oil control (n=4)
Tumor Volume (mm3)
Days After Tumor Implantation

Figure 19. Tumor growth in advanced liver fibrosis following CCl4 continuation and cessation.

A. Schematic experimental design of tumor implantation in murine model of liver fibrosis. Mice underwent the standard CCl_4/oil treatment regimen (Fig. 2A) for up to 12-16 weeks. Mice were assessed for responses to tumors either with implantation at ai) week 12: the peak of liver fibrosis at week ≈12, or at aii) week 16: after 4 weeks of CCl_4 continuation or cessation and when $CD8^+$ T cells were hyperfunctional. Mice were challenged with MC38 a colon adenocarcinoma cell line subcutaneously (s.c. in the right flank of the abdomen with $1x10^5$, $3x10^5$, or $1x10^6$ cells, at the peak of liver fibrosis week 12 (studies B, C, and F). In different studies, treated mice were divided into two groups with CCl_4 continuation or stoppage up to 16 or 20 weeks, (studies B, and D respectively) and then challenged with MC38 cancer cells. **B.** CCl_4 cessation, **C.** CCl_4 continuation. Female mice were injected with MC38 ($1x\ 10^5$) cells at the peak of liver fibrosis (week 12). Tumor growth was bigger in stopped-CCl_4 mice (in red) than in the control (in black), and it was greater in continuous-CCl_4 mice (in red) than stopped-CCl_4. **D.** A higher dose ($3\ x\ 10^5$) of MC38 cells was injected in female mice at the peak of liver fibrosis (week 12). Data are presented as (mean ±SEM), statistical analysis determined using (*$p<0.05$, or **$p<0.001$) a two way ANOVA to compare tumor volume in CCl_4-treated mice vs. control mice.

3.6.b. Immune checkpoint blockade in advanced liver fibrosis

To evaluate responses to immunotherapy, a high dose tumor challenge was conducted. Tumor measurement confirmed that a dose of 1 x 10^6 cells of MC38 resulted in an equivalent growth and size of tumors in both the controls and CCl_4-treated mice, thereby facilitating the comparison of responses to immunotherapy. With the highest dose of MC38 cancer cells (1 x 10^6), five days post-implantation, tumors grew rapidly in both CCl_4-treated mice and the control mice, reaching almost the same size (volume ≈75 mm^3). Then, both groups of mice were injected with the immunotherapy (anti-PD1 + anti-CTLA-4 antibodies) every two days for a total of three-injections. The response to the checkpoint inhibitors in the control group (four mice) started after the second injection of the immunotherapy. After the completion of the immunotherapy injections, the tumor size was reduced and nearly undetectable 16 days post-implantation, after the completion of the immunotherapy injections. In CCl_4-treated mice, however, there was a delayed response to PD-1+CTLA-4 antibodies, with tumor size regressing only after the 3rd injections. Moreover, by the experimental endpoint, 16 days post-implantation, the tumor volume reduced to ≈25 mm^3 in fibrotic mice. This suggests that advanced liver fibrosis and its systemic CD8+ dysfunction is associated not only with impaired control of tumor growth but also delayed responses to immunotherapy (Fig. 20).

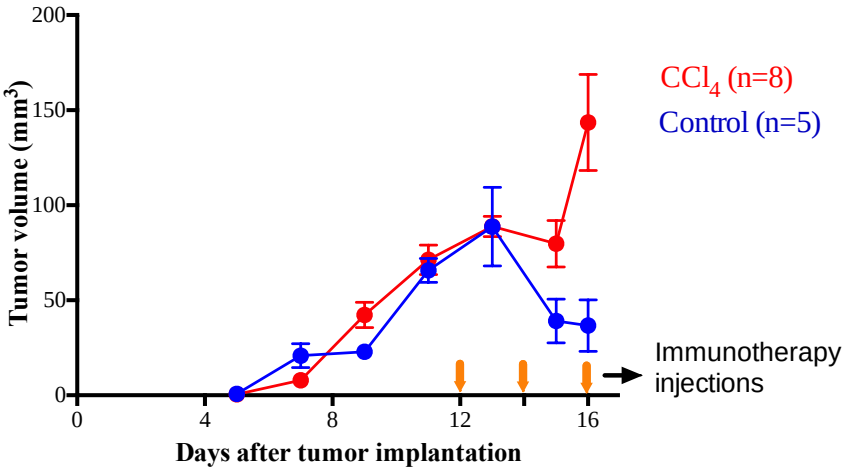
200
150
100
50
0
Tumor volume (mm3)
0
4
8
12
16
Days after tumor implantation
CCl4 (n=8)
Control (n=5)
Immunotherapy
injections

Figure 20. Sustained liver insult accelerates ectopic tumor growth.

When tumor size and volume (≈75 mm^3) were similar, CCl_4- treated mice (n=5) and control mice (n=4) were injected with anti-PD1 + anti-CTLA-4 checkpoint inhibitor antibodies every two days with three injections total. While the control mice responded to the immunotherapy after the first injection, there were delayed response in CCl_4- treated mice.

CHAPTER 4: DISCUSSION

We have developed a CCl_4-induced murine model of advanced liver fibrosis to investigate the phenotype and functions of circulating $CD8^+$ T cells. Our data show that we can successfully induce advanced fibrosis in the C57BL/6 strain and that this is reversible within four-weeks of CCl_4 cessation. In addition, peripheral $CD8^+$ T cells are hyperfunctional in this model, which characterized by elevated induction of IFN-γ^+ and $GrzB^+$ $CD8^+$ T cells in circulation as well as their subsets, particularly naïve and central memory $CD8^+$ T cells. As we have shown in our CCl_4-treated mouse model, this hyperfunctional state is a hallmark of impaired $CD8^+$ T cell functions, resulting in poor responses to tumor growth and immunotherapy *in vivo* in comparison to controls; moreover, it is worse with ongoing liver insult.

4.1. Inducing advanced liver fibrosis in C57BL/6 murine model

Liver fibrosis was induced in mice by administrating the hepatotoxin CCl_4 (1.0 ml/kg) in C57BL/6 mice (i.p.) for up to 12-16 weeks as previously described[93], and mice were able to handle this long-term treatment without any significant mortality (32 weeks). We used the C57BL/6 strain of mice due to the availability of many transgenic lines that would allow us to conduct more mechanistic studies in the future. Although some literature indicated the C57BL/6 mouse strain develops a mild to intermediate fibrosis severity in response to CCl_4 treatment for up to 8-12 weeks[26,55,93,113], we found advanced liver fibrosis can be induced in C57BL/6 mice in both sexes, and all mice achieved advanced liver fibrosis (F3/4) after this prolonged treatment period. Furthermore, treated mice developed advanced fibrosis tolerably and consistently across six independent studies conducted in this thesis research project.

Liver fibrosis regression was also measured in this model in two independent studies, one with female mice and the other with male and female mice. With 12 weeks of exposure to the hepatotoxin, followed by four-weeks of CCl_4 cessation, it was evident liver fibrosis severity reversed to minimal levels (F1), while fibrosis severity was maintained with continued exposure to the liver insult (F3/4). It is also worth noting that these results were observed in females as well as males. This data is consistent with a report in rats that showed spontaneous recovery from CCl_4-induced liver fibrosis after cessation within 28 days, marked by decreased levels of collagen, fibrotic tissue degranulation, and increased apoptosis of activated HSCs in the liver[40]. Our results indicate that advanced fibrosis in this strain of mice (C57BL/6) is reversible within four weeks after administrating CCl_4 for 12 weeks. However, in study E, when male and female mice were treated for prolonged periods of time with the hepatotoxin (16 weeks) and livers were collected at 8-16 weeks post CCl_4 cessation and continuation, sex differences were observed in terms of liver fibrosis regression. In this study, liver fibrosis significantly regressed to F1 in three out of four male mice. In contrast, fibrosis severity remained intermediate in half of the female mice with F2 (n=2) or F3 (n=2) 8-16 weeks after the removal of the liver insult. It is difficult to explain why fibrosis severity was still higher in female mice after CCl_4 cessation than male mice in the same study or the previous one, where advanced fibrosis was regressed in females to control levels (study B). Nevertheless, this persisted fibrosis in females (study E) might be because of the prolonged period of exposure to CCl_4, where mice were administered CCl_4 for longer than 12 -weeks. It has been proposed that the reversibility of cirrhosis depends on the level of fibrotic matrix in advanced or end-stage cirrhotic liver tissue in CCl_4 -induced fibrosis in the rat model. Specifically, the remodelling of liver tissue following cirrhosis in rats administered CCl_4 for eight weeks is histologically different (early micronodular) compared to those treated for 12 weeks

(micronodular) up to 366 days post CCl_4 cessation. Moreover, the recovery from cirrhosis in rats administered CCl_4 for up to 12 weeks is incomplete after 366-days after CCl_4-cessation[41]. In humans, fibrosis/cirrhosis regression depends on the severity of fibrosis and the time of viral elimination. For instance, there is a possibility for cirrhotic compensated patients with HCV infection to regress to F3, but it is irreversible in decompensated cirrhosis, stromal patients with vascular alteration[29].

Moreover, in study E, with CCl_4 continuation for up to 16 weeks, we show for the first time the novelty of this CCl_4 murine model in terms of handling the hepatotoxin (1 ml/kg twice/week) to induce advanced liver fibrosis while tolerating the hepatotoxin for extended periods of time (~30 weeks) without any observation of morbidity or mortality. Previous studies indicated increased mortality and differences in weight gains in rats between the CCl_4-treated group and the controls[1,24].

4.2. Associated hyperfunctional $CD8^+$ T cells with advanced liver fibrosis

$CD8^+$ T cells play a crucial role in cell-mediated antiviral response to HCV infection[108,115,79,78]; however, it is not known yet why the majority of HCV^+ individuals fail in the clearance of the virus. The impairment and terminal exhaustion of HCV-specific $CD8^+$ T cell responses has been reported in several liver diseases, particularly in HCV^+ individuals[115]. While many publications have focused on HCV-infected individuals with minimal liver fibrosis, some have reported immune cell dysfunction in HCV infection with cirrhosis[62,13]. Furthermore, we and others have reported generalized $CD8^+$ T cell hyperfunction in HCV^+ infection with advanced fibrosis[111,2]. This project showed that circulating $CD8^+$ T cell functions at the peak of CCl_4-induced liver fibrosis in mice were marked by elevated IFN-γ^+ and $GrzB^+$ bulk $CD8^+$ T cells. This elevation was observed after 12 weeks of CCl_4 treatment compared to the control mice, yet no significant

changes were observed in earlier weeks of treatment, except for one study showing high induction of $GrzB^+$. These results were seen repeatedly in six independent studies, suggesting a strong association between bulk $CD8^+$ T cell hyperfunction and advanced liver fibrosis though the mechanisms are still unknown. Similarly, in a CCl_4-induced cirrhosis rat model, a general activation of monocytes, B and T cells, an alteration in the phenotype of circulating T cells in cirrhotic rats after 12-18 weeks of the exposure to CCl_4, as well as a significant elevation in the production of IFN-γ^+ on circulating T helper cells upon activation in cirrhotic rats was observed. Also, there was an elevation in the induction of pro-inflammatory TNF-α on monocytes and DCs in cirrhotic mice compared to the controls rats[118,72,71]. These data suggest chronic liver insult-induced cirrhosis is associated with dysfunctional innate and adaptive immune cells that compromise the host immune system.

4.3. CD8+ T cell subsets contributing to immune hyperfunction in advanced liver fibrosis

We investigated the function of $CD8^+$ T cell subsets in a murine model of advanced liver fibrosis. Interestingly, we found that naïve and central memory $CD8^+$ T cells were the most contributing subsets in circulating $CD8^+$ T cell hyperfunction in advanced liver fibrosis. Reported initially in 2015, there was an alteration in the phenotyping of naïve and memory-like bulk $CD8^+$ T cells in chronic HCV-infected individuals in comparison to healthy or treated individuals who were, hyperactive to TCR signalling[2]. The Crawley lab also reported pronounced hyperfunction in naïve $CD8^+$ T cells in humans[111]. Specifically, there was an elevation in the production of the pro-inflammatory IFN-γ^+ and the degranulation marker $CD107a^+$ $CD8^+$ T cells in chronic HCV-infected individuals with advanced liver fibrosis after DAA treatment. This hyperactivation of non-specific T cells in chronic liver disease implies biological "distraction" for circulating immune cells, resulting in impaired immune responses against antigen-specific HCV infection and tumors.

Therefore, advanced liver fibrosis has a negative impact on $CD8^+$ T cell functions, specifically naïve $CD8^+$ T cells. However, the mechanisms of this activation need to be elucidated more in the future.

The Crawley lab has reported the influence of the liver stage on circulating $CD8^+$ T cell functions in HCV infection. In 2016, an association was shown between anti-apoptotic molecule Bcl-2 expression and liver fibrosis severity in response to IL-7 stimulation, wherein HCV-infected individuals with advanced liver fibrosis (F3/4) produced significantly less Bcl-2 compared to those with minimal fibrosis (F1/2)[92]. In 2019, it was reported that non-specific $CD8^+$ T cells were hyperfunctional in HCV patients with advanced liver fibrosis compared to minimal fibrosis, marked by significant expression of IFN-γ^+, $CD107a^+$, and perforin. Notably, this phenomenon of hyperfunction remained even after DAA treatment. Moreover, preliminary RNA-sequencing analyses in the lab indicate significant differences in expression of over 400 genes after stimulation of bulk $CD8^+$ T-cells *in vitro* in treated-naïve HCV-infected individuals with minimal liver fibrosis in comparison to cirrhotic individuals, suggesting the link between the severity of liver fibrosis and $CD8^+$ T cell gene expression patterns. Those genes were involved in apoptosis, cell cycling, metabolism, replication, and activation. The pattern of those gene expressions was persistent post antiviral therapy, confirming that chronic HCV infection with cirrhosis results in long-lasting dysfunctional $CD8^+$ T cells. According to unpublished data, the hyperfuntional IFN-$\gamma^{+,}$ and $GrzB^+$ $CD8^+$ T cells in HCV-infected individuals with advanced liver fibrosis are showing signs of apoptosis as measured by Caspase 3 and Annexin-V detection following treatment with apoptosis-inducing Fas ligand (Crawley, unpublished). This supports previous reports that HCV infection is associated with increased apoptosis of hepatocytes and HCV-specific CD8 T cells as well as apoptosis of activated peripheral B, $CD4^+$ and $CD8^+$ T cells [39,20,61].

4.4. Activation markers of CD8 T cells in advanced liver fibrosis

It is well documented that activation and inhibitory markers highly regulate $CD8^+$ T cell responses against viral infection, particularly HCV infection. Nakamoto et al. reported that HCV-specific cytotoxic T lymphocytes in circulation showed an elevation of inhibitory receptors such as PD-1 and CTLA-4[74]. However, in our model of advanced liver fibrosis, we did not observe any change in PD-1 expression in bulk $CD8^+$ T cells between the CCl_4-treated mice and the controls. This was confirmed in a recent study that showed no elevation of exhaustion markers on bulk T populations in HCV individuals with advanced liver fibrosis[76].

The activation marker NKG2D is induced on the surface of cytotoxic $CD8^+$ T cells in response to stressors or following TCR activation[84]. NKG2D acts as a CD28 co-stimulatory receptor to boost T cell function upon TCR activation[42]. NKG2D ligands are expressed on many tumor cell lines, and they mediate immune surveillance of melanoma, suggesting the involvement of the NKG2D receptor in anti-tumor immunity. NKG2D expression was assessed in our model of advanced liver fibrosis, and was significantly and unexpectedly lower in CCl_4-treated mice upon *in vitro* TCR stimulation compared to the control mice. This significant reduction in fibrotic mice was seen repeatedly in a few studies. It was reported that downregulated NKG2D expression was also observed on circulating $CD8^+$ T cells in gastric cancer patients compared to the controls, and this is further associated with $CD8^+$ T cell impairment against tumors[77]. It was also shown that NKG2D ligand plays a role in restoring $CD8^+$ T cells functions in the absence of helper T cells[84]. In a recent study, tumor growth was significantly reduced in mice by targeting $NKG2D^+$ T cells, suggesting the use of NKG2D signalling as a new immunotherapeutic due to its wide expression on malignancies[19]. These results of significantly reduced NKG2D expression on circulating $CD8^+$

T cells may be used as a hallmark of dysfunctional and impaired $CD8^+$ T cells in advanced liver fibrosis, yet the mechanisms are still not known.

4.5. Sustained hyperfunction of $CD8^+$ T cell in severe fibrosis after liver insult removal

Liver fibrosis in HCV^+ infected individuals might or might not regress, depending on the severity. Those with low severity are more likely to regress to F1, while other with advanced liver fibrosis or cirrhotic-infected individuals with HCV may not experience any improvement at all [73]. It was shown in a previous report that HCV^+ individuals with advanced liver fibrosis had hyperfunctional bulk $CD8^+$ T cells compared to those with minimal fibrosis, and that this is long-lasting even after DAA antiviral therapy. To be specific, the proportion of IFN-γ, CD107a, and perforin remained significantly elevated in those with advanced fibrosis in comparison with minimal and healthy donors[111]. In the CCl_4 mouse model, liver fibrosis regressed from F3/4 to F1/2, compared to the control mice within four weeks, and interestingly, $CD8^+$ T cells remained hyperfunctional long after CCl_4 cessation, expressing a high percentage of $GrzB^+$, IFN-γ^+, and $CD107a^+$ $CD8^+$ T cells in CCl_4-treated mice eight weeks post-cessation. This implies that the impact of chronic liver insult results in long-lasting hyperfunctional bulk $CD8^+$ T cells. In chronic LCMV infection in mice, it was reported that exhausted T cell subsets had a distinct transcriptional and epigenetic landscape and because they were terminally dysfunctional and genetically imprinted, they failed in the response against viral infection and cancer growth. Therefore, prolonged exposure to liver insult results in sustained hyperfunctional $CD8^+$ T cells, particularly in GrzB expression, degranulation, and activation, and this hyper-functionality may not be reversible in mice or humans. This mimics the retention of $CD8^+$ T cell hyperfunction observed in DAA-treated HCV^+ individuals with cirrhosis, implying cirrhotic individuals are at elevated risk of having poor immune responses.

4.6. Sex differences in a mouse model of advanced liver fibrosis

Sex effects have been reported in several liver diseases such as NAFLD[91], HBV[38], HCV[52,8,83], and HCC[117]. It has been reported that the rate of liver fibrosis progression in women is ten times less than in men[22]. In our mouse models, the initial hyperfunction of $CD8^+$ T cells was observed and conducted in females. When a small group of males was included in the preceding experiment, some previously reported differences were seen, suggesting sex effects in this murine model[7]. For the first time, we closely studied the sex effect in the CCl_4-induced advanced liver fibrosis model. In terms of body weight, both sexes briefly lost less than 10% of their body weight when the CCl_4 treatment was initiated. However ,while there was a slight, transient drop in the bodyweight of female CCl_4-treated mice at weeks two to three.. The female mice regained weight to equal that of the controls. Male CCl_4-treated mice, however, started to lose weight slightly at weeks six, and did not regain weight to control levels over time though they did yet continue to gain weight at the same rate. The initial signs of hyperfunction of $CD8^+$ T cells observed in this model were conducted in females. When a small group of males was included in the previous study, some differences between the sexes were observed, suggesting there are sex effects in this murine model. We found some changes in the hyperfunctional $CD8^+$ T cells in terms of sex effect, wherein the induction of $GrzB^+$ cells was significantly higher in fibrotic female mice but not in males. On the other hand, IFN-γ^+ production in male mice that stopped receiving CCl_4 was greater than the controls. The pathology analyses of all mice in these studies confirmed that there are no differences in liver fibrosis progression and the severity of fibrosis between the sexes. However, only study E showed fibrosis regression might be faster in males than females. Nevertheless, it is still challenging to determine the association between sex and the degree of $CD8^+$ T cell hyperfunctions in mice with advanced liver fibrosis because although we did the experiment twice,

the data did not agree. The data implies there might be some effects, so further study is needed to understand sex effects in liver diseases better.

4.7. Tumor growth in advanced liver fibrosis

We measured the response of hyperfunctional $CD8^+$ T cells to tumor growth and immunotherapy in CCl_4-induced advanced liver fibrosis *in vivo* in mice. We showed that tumor out-growth was more rapid in fibrotic mice compared to the controls, and it was significantly greater in continued CCl_4 mice compared to those after CCl_4 cessation. As discussed earlier, as a consequence of chronic liver fibrosis, $CD8^+$ T cell hyperfunction shows abnormal functions, characterized by high induction of pro-inflammatory cytokines and significant reduction of activation markers, which suggests these cells are impaired. Tumor growth strongly indicates that severe fibrosis not only has a negative impact on host immune response, resulting in larger and faster tumor growth, but also that a state of $CD8^+$ T cells hyperfunction is associated with cancer growth in fibrotic mice through unknown mechanisms. Moreover, continued liver insult exacerbates this association, particularly in cirrhotic HCV-infected individuals who are at the highest risk of having HCC. These data confirm that individuals with advanced liver fibrosis might suffer such impaired specific immune responses mediated by $CD8^+$ T cells resulting in rapid tumor growth and delayed response to immunotherapy.

To conclude, our project of advanced liver fibrosis murine model shows that cytotoxic $CD8^+$ T cells are hyperfunctional marked by elevated induction of IFN-γ and GrzB in the circulation in liver-insult induced liver fibrosis. This indicates the association between the stage of liver fibrosis and $CD8^+$ T cell hyperfunction, which is a hallmark of dysregulated immune cells. This associated dysregulation of immune cells with advanced liver fibrosis has been reported by our lab and others in cirrhotic individuals with HCV infection even after being cured with antiviral

therapy. This highlights the severe consequences of immunodeficiency and liver complications such as liver decompaction, hepatocellular carcinoma, liver failure or death that cirrhotic HCV-infected individuals might suffer. Furthermore, we showed these dysregulated $CD8^+$ T cells failed in the clearance of tumor cells and poor responses to immunotherapy. This implies that advanced fibrosis impacts not only the immune responses of individuals with HCV infection but also that they face a high risk of impaired specific immune responses to co-infection or hepatocellular carcinoma. This might explain why some individuals with chronic liver diseases are poor candidates for immunotherapy unless we can find a way to restore their immunity.

CHAPTER 5: FUTURE DIRECTIONS

In this project, we established advanced liver fibrosis in a C57BL/6 murine model of hepatotoxin-mediated chronic liver injury, to assess the responsiveness of peripheral $CD8^+$ T cells during fibrosis progression and at the peak of liver disease severity. Our most important findings are that circulating $CD8^+$ T cells are hyperfunctional, marked byelevated IFN-γ and GrzB expression in advanced liver fibrosis compared to the controls. More interestingly, naïve and central memory $CD8^+$ T cells were significant contributors to this hyperfunction. It is unknown yet whether this phenomenon would be replicated in aetiologies of advanced chronic liver disease such as those with fatty liver disease. Moreover, it is questionable whether these hyperfunctioanl $CD8^+$ T cells are still proliferative when triggered by antigen exposure and an immune response, particularly given the outcomes of the tumour challenge in this study. This can be addressed by conducting *in vitro* proliferation assays of cytotoxic $CD8^+$ T cells after 12 weeks of treatment with the hepatotoxin CCl_4. Elevated markers of apoptosis in $CD8^+$ T cell has been reported in chronic diseases such as HBV, HCV, and HIV[39,20,61]. It would be valuable to observe whether these hyperfunctional $CD8^+$ T cells are also apoptotic and dying in our murine model of advanced liver fibrosis.

If we find that $CD8^+$ T cells are less proliferative in fibrotic mice as expected, then we could adjust the panel and add some exhaustion markers to study whether those hyperfunctional T cells are also exhausted using additional markers alongside PD-1. For example, add exhaustion markers CD39 and Tim3 while removing markers from the current panel in which no changes between treated mice and the controls were observed (e.g. CD107a, NKG2D, TNF-α). Exhaustion markers can be a potential strategy to restore T cell functions in chronic liver disease. Moreover,

it is possible to study other functions, activation, or phenotyping markers of $CD8^+$ T cells in the future by adding markers of interest to the panel.

We and others reported liver fibrosis regression in a CCl_4-induced advanced fibrosis murine model after 12 weeks of the treatment. However, another unexpected finding was the sex difference in liver fibrosis regression after a prolonged period of 8-16 weeks post liver insult cessation. Unlike an earlier study in which advanced liver fibrosis was reversed to F1 in females four weeks post CCl_4 cessation, in larger cohort of mice, we found advanced fibrosis persisted in females after 8-16 weeks post liver insult removal compared to the controls and males. This suggests longer periods of liver insult results in irreversible severe fibrosis. However, we did not do this experiment more than once and it was limited by a small number of mice. It would be interesting to repeat it in a larger number of mice to confirm this finding.

The use of the CCl_4 model has some limitations that should be acknowledged. The duration of establishing fibrosis in this model, taking around 8-12 weeks to induce advanced fibrosis in mice, prevents us from addressing some research questions in isolation. Due to a shortage of time and the number of mice, we tried to address two research questions simultaneously, assessing fibrosis regression and tumor growth in an advanced liver fibrosis model. Although we did our best to evaluate fibrosis regression after tumor implantation, livers were harvested when mice reached the end point (i.e. peak tumor volume), so some livers had a longer time to reverse than others. Therefore, it would be better in the future if all livers were collected and scored at the same time to eliminate any unnecessary variations.

Sustained hyperfunction of $CD8^+$ T cell in advanced liver fibrosis eight weeks post liver insult removal is an important aspect in this project of CCl_4-induced advanced liver fibrosis. This was after mice were treated with CCl_4 for 19 - 21 weeks. However, if we had more mice, it would

have been better to first study whether the hyperfunction of $CD8^+$ T cells is reversible once it was observed at week 12 of the CCl_4 treatment. For instance, mice could be bled two- and four-weeks post CCl_4-continuation or cessation to determine how long the state of hyperfunctional $CD8^+$ T cells would last with and without the hepatotoxin. Then, we could aim for longer periods with the treatment. It might show whether chronic liver insult results in long lasting dysfunctional $CD8^+$ T cells, or not. Such information will build our knowledge about our mouse model of advanced fibrosis and chronic liver disease.

Hyperfunction of $CD8^+$ T cells is a hallmark of immune cell dysregulation in advanced liver fibrosis. Our research showed that dysfunctional $CD8^+$ T cells were not able to control tumor growth *in vivo;* additionally, the responses to immunotherapy were poor in our model of advanced liver fibrosis compared to the controls. Indeed, sex differences have been a struggle in studying tumor growth *in vivo* in the murine model of advanced fibrosis. In our preliminary data, we used the MC38 tumor cell line, which was originally derived from a female mouse in a cohort of female mice and the results showed a clear difference in tumor growth between CCl_4-treated mice and the controls. However, when we had another cohort of mice of both sexes, the difference of tumor growth between the two groups was affected, and we speculate that this is due to the tumor cell line used. We tried to use a male-derived B16F10 tumor cell line, but the result was not as noticeable as it was in females. Since these are two completely different cell lines, more optimization for the B16F10 cell line is required to adequately evaluate any potential sex effects in this model.

REFERENCES

1. A D, HM M. Efficient tissue repair underlies the resiliency of postnatally developing rats to chlordecone + CCl4 hepatotoxicity. *Toxicology*. 1996;111(1-3):29-42. doi:10.1016/0300-483X(96)03391-4

2. Alanio C, Nicoli F, Sultanik P, et al. Bystander hyperactivation of preimmune CD8+ T cells in chronic HCV patients. *Elife*. 2015;4(Lcmv):1-20. doi:10.7554/elife.07916

3. Alao H, Cam M, Keembiyehetty C, et al. Baseline Intrahepatic and Peripheral Innate Immunity Are Associated With Hepatitis C Virus Clearance During Direct-Acting Antiviral Therapy. 2018;68(6). doi:10.1002/hep.29921/suppinfo

4. Albillos A, Lario M, Álvarez-Mon M. Cirrhosis-associated immune dysfunction: Distinctive features and clinical relevance. *J Hepatol*. 2014;61(6):1385-1396. doi:10.1016/j.jhep.2014.08.010

5. Ann Liebert M, Kato N. *Review Genome of Human Hepatitis C Virus (HCV): Gene Organization, Sequence Diversity, and Variation*. Vol 5.; 2000. www.liebertpub.com

6. Asrani SK, Devarbhavi H, Eaton J, Kamath PS. Burden of liver diseases in the world. *J Hepatol*. 2019;70(1):151-171. doi:10.1016/J.JHEP.2018.09.014

7. Aydos LR, Aparecida Do Amaral L, Serafim De Souza R, et al. Nonalcoholic Fatty Liver Disease Induced by High-Fat Diet in C57bl/6 Models. Published online 2019. doi:10.3390/nu11123067

8. Bakr I, Rekacewicz C, Hosseiny E, et al. Higher clearance of hepatitis C virus infection in females compared with males. *Gut*. 2006;55:1183-1187. doi:10.1136/gut.2005.078147

9. Bastidas S, Graw F, Smith MZ, Kuster H, Günthard HF, Oxenius A. CD8 + T Cells Are Activated in an Antigen-Independent Manner in HIV-Infected Individuals . *J Immunol*. 2014;192(4):1732-1744. doi:10.4049/jimmunol.1302027

10. Bentham J, Di Cesare M, Bilano V, et al. Worldwide trends in body-mass index, underweight, overweight, and obesity from 1975 to 2016: a pooled analysis of 2416 population-based measurement studies in 128·9 million children, adolescents, and adults. *Lancet*. 2017;390(10113):2627-2642. doi:10.1016/S0140-6736(17)32129-3

11. Buzzetti E, Lombardi R, De Luca L, Tsochatzis EA. Noninvasive Assessment of Fibrosis in Patients with Nonalcoholic Fatty Liver Disease. Published online 2015. doi:10.1155/2015/343828

12. Chen M, Hu P, Peng H, et al. Enhanced Peripheral γδT Cells Cytotoxicity Potential in Patients with HBV-Associated Acute-On-Chronic Liver Failure Might Contribute to the Disease Progression. *J Clin Immunol*. 2012;32:877-885. doi:10.1007/s10875-012-9678-z

13. Clària J, Mitchell DA, Irvine KM, Ratnasekera I, Powell EE, Hume DA. Causes and Consequences of Innate Immune Dysfunction in Cirrhosis. *Front Immunol | www.frontiersin.org*. 2019;10:293. doi:10.3389/fimmu.2019.00293

14. Cousineau SE, Erman A, Liu L, et al. The 8 th Canadian Symposium on Hepatitis C virus: "Improving diagnosis and linkage to care" . *Can Liver J*. 2020;3(1):3-14. doi:10.3138/canlivj.2019-0032

15. Craig. immune surveillance by the liver. *Jenne* . Published online 2013:1-11. doi:10.1038/ni.2691

16. Dahari H, Feliu A, Garcia-Retortillo M, Forns X, Neumann AU. Second hepatitis C replication compartment indicated by viral dynamics during liver transplantation. *J Hepatol*. 2005;42(4):491-498. doi:10.1016/j.jhep.2004.12.017

17. Delire B, Stärkel P, Leclercq I. Animal Models for Fibrotic Liver Diseases: What We Have, What We Need, and What Is under Development. Published online 2015. doi:10.14218/JCTH.2014.00035

18. Dikopoulos N, Wegenka U, Kröger A, et al. Recently Primed CD8 T Cells Entering the Liver Induce Hepatocytes to Interact With Naı¨veNaı¨ve CD8 T Cells in the Mouse. Published online 2004. doi:10.1002/hep.20173

19. Driouk L, Gicobi JK, Kamihara Y, et al. Chimeric Antigen Receptor T Cells Targeting NKG2D-Ligands Show Robust Efficacy Against Acute Myeloid Leukemia and T-Cell Acute Lymphoblastic Leukemia. doi:10.3389/fimmu.2020.580328

20. E T, A K, L G, et al. Enhanced peripheral T-cell apoptosis in chronic hepatitis C virus infection: association with liver disease severity. *J Hepatol*. 2001;35(6):774-780. doi:10.1016/S0168-8278(01)00207-0

21. Efremova M, Rieder D, Klepsch V, et al. Targeting immune checkpoints potentiates immunoediting and changes the dynamics of tumor evolution. *Nat*

Commun. 2018;9(1). doi:10.1038/s41467-017-02424-0

22. Fabio SB, Enrica N, Alessandra B, Dante M, Lonardo RA. NAFLD as a Sexual Dimorphic Disease: Role of Gender and Reproductive Status in the Development and Progression of Nonalcoholic Fatty Liver Disease and Inherent Cardiovascular Risk. *Adv Ther*. 2017;34. doi:10.1007/s12325-017-0556-1

23. Ferrell L. *Liver Pathology: Cirrhosis, Hepatitis, and Primary Liver Tumors. Update and Diagnostic Problems*.; 2000.

24. Fortea JI, Fernández-Mena C, Puerto M, et al. Comparison of Two Protocols of Carbon Tetrachloride-Induced Cirrhosis in Rats-Improving Yield and Reproducibility. Published online 2015. doi:10.1038/s41598-018-27427-9

25. Friedman SL, Neuschwander-Tetri BA, Rinella M, Sanyal AJ. Mechanisms of NAFLD development and therapeutic strategies. *Nat Med*. Published online 2018. doi:10.1038/s41591-018-0104-9

26. Fujii T, Fuchs BC, Yamada S, et al. *Mouse Model of Carbon Tetrachloride Induced Liver Fibrosis: Histopathological Changes and Expression of CD133 and Epidermal Growth Factor*.; 2010. http://www.biomedcentral.com/1471-230X/10/79

27. Gao B. Basic liver immunology. *Cell Mol Immunol*. 2016;13:265-266. doi:10.1038/cmi.2016.9

28. Gao H-Y, Li G-Y, Lou M-M, Li X-Y, Wei X-Y, Wang J-H. *Hepatoprotective Effect of Matrine Salvianolic Acid B Salt on Carbon Tetrachloride-Induced Hepatic Fibrosis*.; 2012. http://www.journal-inflammation.com/content/9/1/16

29. Garcia-Tsao G. *Preventing Infections?*; 2019.

30. Gerold G, Pietschmann T. E-Mail The HCV Life Cycle: In vitro Tissue Culture Systems and Therapeutic Targets. *Dig Dis*. 2014;32:525-537. doi:10.1159/000360830

31. Giannini EG, Testa R, Savarino V. Liver enzyme alteration: A guide for clinicians. *Cmaj*. 2005;172(3):367-379. doi:10.1503/cmaj.1040752

32. Grakoui A, Crispe IN. Presentation of hepatocellular antigens. Published online 2016. doi:10.1038/cmi.2015.109;published

33. Haas A, Zimmermann K, Graw F, et al. Systemic antibody responses to gut commensal bacteria during chronic HIV-1 infection. *Gut*. 2011;60(11):1506-

1519. doi:10.1136/GUT.2010.224774

34. Haas A, Zimmermann K, Oxenius A. Antigen-Dependent and-Independent Mechanisms of T and B Cell Hyperactivation during Chronic HIV-1 Infection. *J Virol*. 2011;85(23):12102-12113. doi:10.1128/JVI.05607-11

35. Hardy T, Oakley F, Anstee QM, Day CP. Nonalcoholic Fatty Liver Disease: Pathogenesis and Disease Spectrum. *Annu Rev Pathol Mech Dis*. 2016;11:451-496. doi:10.1146/annurev-pathol-012615-044224

36. Highton AJ, Schuster IS, Degli-Esposti MA, Altfeld M. The role of natural killer cells in liver inflammation. doi:10.1007/s00281-021-00877-6

37. Horst AK, Neumann K, Diehl L, Tiegs G. Modulation of liver tolerance by conventional and nonconventional antigen-presenting cells and regulatory immune cells. *Cell Mol Immunol*. 2016;13:277-292. doi:10.1038/cmi.2015.112

38. Hsieh A-R, Fann CS, Yeh C-T, et al. Effects of sex and generation on hepatitis B viral load in families with hepatocellular carcinoma. *World J Gastroenterol*. 2017;23(5):876. doi:10.3748/WJG.V23.I5.876

39. Iken K, Huang L, Bekele H, Schmidt E V., Koziel MJ. Apoptosis of activated CD4+ and CD8+ T cells is enhanced by co-culture with hepatocytes expressing hepatitis C virus (HCV) structural proteins through FasL induction. *Virology*. 2006;346(2):363-372. doi:10.1016/j.virol.2005.11.017

40. Iredale JP, Benyon RC, Pickering J, et al. *Mechanisms of Spontaneous Resolution of Rat Liver Fibrosis Hepatic Stellate Cell Apoptosis and Reduced Hepatic Expression of Metalloproteinase Inhibitors*. Vol 102.; 1998. http://www.jci.org

41. Issa R, Zhou X, Constandinou CM, et al. Spontaneous recovery from micronodular cirrhosis: Evidence for incomplete resolution associated with matrix cross-linking. *Gastroenterology*. 2004;126(7):1795-1808. doi:10.1053/j.gastro.2004.03.009

42. Jamieson AM, Diefenbach A, McMahon CW, Xiong N, Carlyle JR, Raulet DH. The role of the NKG2D immunoreceptor in immune cell activation and natural killing. *Immunity*. 2002;17(1):19-29. doi:10.1016/S1074-7613(02)00333-3

43. JJ M, N A, SB K, et al. Studying Immunotherapy Resistance in a Melanoma Autologous Humanized Mouse Xenograft. *Mol Cancer Res*. 2020;19(2):346-357. doi:10.1158/1541-7786.MCR-20-0686

44. John Wherry E, Kurachi M. Molecular and cellular insights into T cell exhaustion. *Nat Publ Gr*. Published online 2015. doi:10.1038/nri3862

45. Ju C, Tacke F. Hepatic macrophages in homeostasis and liver diseases: from pathogenesis to novel therapeutic strategies. Published online 2016. doi:10.1038/cmi.2015.104;published

46. Kalra A, Tuma F. *Physiology, Liver*. StatPearls Publishing; 2018. Accessed March 4, 2021. http://www.ncbi.nlm.nih.gov/pubmed/30571059

47. Kanwal F, Kramer JR, Duan Z, et al. Trends in the Burden of Nonalcoholic Fatty Liver Disease in a United States Cohort of Veterans. Published online 2016. doi:10.1016/j.cgh.2015.08.010

48. Khullar V, Firpi RJ. Hepatitis C cirrhosis: New perspectives for diagnosis and treatment. *World J Hepatol*. 2015;7(14):1843. doi:10.4254/WJH.V7.I14.1843

49. Kish T, Aziz A, Sorio M. *Hepatitis C in a New Era: A Review of Current Therapies*. Vol 42.; 2017.

50. Koo S-Y, Park E-J, Lee C-W. Immunological distinctions between nonalcoholic steatohepatitis and hepatocellular carcinoma. *Exp Mol Med*. Published online 2020. doi:10.1038/s12276-020-0480-3

51. Kubes P, Jenne C. Immune Responses in the Liver. *Annu Rev Immunol*. 2018;36:247-277. doi:10.1146/annurev-immunol-051116-052415

52. Lai JC, Verna EC, Brown RS, et al. Hepatitis C Virus-Infected Women Have a Higher Risk of Advanced Fibrosis and Graft Loss After Liver Transplantation than Men. Published online 2011. doi:10.1002/hep.24390

53. Lakshman R, Shah R, Reyes-Gordillo K, Varatharajalu R. Synergy between NAFLD and AFLD and potential biomarkers. *Clin Res Hepatol Gastroenterol*. 2015;39:S29-S34. doi:10.1016/j.clinre.2015.05.007

54. Le MH, Devaki P, Ha NB, et al. Prevalence of non-alcoholic fatty liver disease and risk factors for advanced fibrosis and mortality in the United States. Published online 2017. doi:10.1371/journal.pone.0173499

55. Liedtke C, Luedde T, Sauerbruch T, et al. Experimental liver fibrosis research: update on animal models, legal issues and translational aspects. *Fibrogenes Tissue Repair 2013 61*. 2013;6(1):1-25. doi:10.1186/1755-1536-6-19

56. Lin Z-H, Xin Y-N, Dong Q-J, et al. Performance of the Aspartate

Aminotransferase-to-Platelet Ratio Index for the Staging of Hepatitis C-Related Fibrosis: An Updated Meta-Analysis. Published online 2011. doi:10.1002/hep.24105

57. Lindenbach BD, Rice CM. INSIGHT REVIEW Unravelling hepatitis C virus replication from genome to function Initial studies: HCV translation and polyprotein processing. Published online 2005. doi:10.1038/nature04077

58. Lisco A, Vanpouille C, Margolis L. War and Peace between Microbes: HIV-1 Interactions with Coinfecting Viruses. *Cell Host Microbe*. 2009;6(5):403-408. doi:10.1016/j.chom.2009.10.010

59. Liu X, Jiang X, Liu R, et al. B Cells Expressing CD11b Effectively Inhibit CD41 T-Cell Responses and Ameliorate Experimental Autoimmune Hepatitis in Mice. Published online 2015. doi:10.1002/hep.28001/suppinfo

60. Lund FE, Randall TD. Effector and regulatory B cells: modulators of CD4 + T cell immunity. *Nat Publ Gr*. Published online 2010. doi:10.1038/nri2729

61. M B, K G, R M, et al. Chronic hepatitis C virus infection triggers spontaneous differential expression of biosignatures associated with T cell exhaustion and apoptosis signaling in peripheral blood mononucleocytes. *Apoptosis*. 2015;20(4):466-480. doi:10.1007/S10495-014-1084-Y

62. M D, AE R. Role of systemic inflammation in cirrhosis: From pathogenesis to prognosis. *World J Hepatol*. 2015;7(16):1974-1981. doi:10.4254/WJH.V7.I16.1974

63. Ma chi, Kesarwala aparna, Eggert T, et al. NAFLD causes selective CD4 + T lymphocyte loss and promotes hepatocarcinogenesis. *Nature*. Published online 2016. doi:10.1038/nature16969

64. McLane LM, Abdel-Hakeem MS, Wherry EJ. CD8 T Cell Exhaustion During Chronic Viral Infection and Cancer. *Annu Rev Immunol*. 2019;37:457-495. doi:10.1146/annurev-immunol-041015-055318

65. Meli R, Raso GM, Calignano A, Gualillo O, Gaetani S. Role of innate immune response in non-alcoholic fatty liver disease: metabolic complications and therapeutic tools. Published online 2014. doi:10.3389/fimmu.2014.00177

66. Michalopoulos GK, Bhushan B. Liver regeneration: biological and pathological mechanisms and implications. *Nat Rev Gastroenterol Hepatol*. 2021;18(1):40-55. doi:10.1038/s41575-020-0342-4

67. Millman AJ, Nelson NP, Vellozzi C. Hepatitis C: Review of the Epidemiology, Clinical Care, and Continued Challenges in the Direct-Acting Antiviral Era. Published online 2017. doi:10.1007/s40471-017-0108-x

68. Mitra V, Metcalf J. Metabolic functions of the liver. *Anaesth Intensive Care Med*. 2009;10(7):334-335. doi:10.1016/j.mpaic.2009.03.011

69. Mohankumar S, Patel T. Extracellular vesicle long noncoding RNA as potential biomarkers of liver cancer. doi:10.1093/bfgp/elv058

70. Moreno BH, Zaretsky JM, Garcia-Diaz A, et al. Response to Programmed Cell Death-1 Blockade in a Murine Melanoma Syngeneic Model Requires Costimulation, CD4, and CD8 T Cells. Published online 2016. doi:10.1158/2326-6066.CIR-16-0060

71. Mu L, Jos Borrero M, Ubeda M, et al. Interaction Between Intestinal Dendritic Cells and Bacteria Translocated From the Gut in Rats With Cirrhosis. *HEPATOLOGY*. 2012;56:1861-1869. doi:10.1002/hep.25854

72. Muñoz L, Albillos A, Nieto M, et al. Mesenteric Th1 polarization and monocyte TNF-α production: First steps to systemic inflammation in rats with cirrhosis. *Hepatology*. 2005;42(2):411-419. doi:10.1002/hep.20799

73. Nahon P, Ganne-Carrié N. Management of patients with pre-therapeutic advanced liver fibrosis following HCV eradication. *JHEP Reports*. 2019;1(6):480. doi:10.1016/J.JHEPR.2019.11.001

74. Nakamoto N, Kaplan DE, Coleclough J, et al. Functional Restoration of HCV-Specific CD8 T Cells by PD-1 Blockade Is Defined by PD-1 Expression and Compartmentalization. *Gastroenterology*. 2008;134(7):1927-1937. doi:10.1053/j.gastro.2008.02.033

75. November ; Michelotti |. NAFLD, NASH and liver cancer. *Nat Rev Gastroenterol Hepatol*. 2013;10:656-665. doi:10.1038/nrgastro.2013.183

76. Okwor CIA, Oh JS, Crawley AM, Cooper CL, Lee SH. Expression of Inhibitory Receptors on T and NK Cells Defines Immunological Phenotypes of HCV Patients with Advanced Liver Fibrosis. *iScience*. 2020;23(9). doi:10.1016/J.ISCI.2020.101513

77. Osaki T, Saito H, Yoshikawa T, et al. Decreased NKG2D Expression on CD8+T Cell Is Involved inImmune Evasion in Patients with Gastric Cancer. *Clin Cancer Res*. 2007;13(2). doi:10.1158/1078-0432.CCR-06-1454

78. Park S-H, Suresh Veerapu N, Shin E-C, et al. Subinfectious hepatitis C virus

exposures suppress T cell responses against subsequent acute infection. *Nat Med*. 2013;19. doi:10.1038/nm.3408

79. Park SH, Rehermann B. Immune responses to HCV and other hepatitis viruses. *Immunity*. 2014;40(1):13-24. doi:10.1016/j.immuni.2013.12.010

80. Parker GA, Picut CA. Invited Review Liver Immunobiology. *Toxicol Pathol*. 2005;33:52-62. doi:10.1080/01926230590522365

81. St. Paul M, Ohashi PS. The Roles of CD8+ T Cell Subsets in Antitumor Immunity. *Trends Cell Biol*. 2020;30(9):695-704. doi:10.1016/j.tcb.2020.06.003

82. Piscaglia F, Svegliati-Baroni G, Barchetti A, et al. Clinical Patterns of Hepatocellular Carcinoma in Nonalcoholic Fatty Liver Disease: A Multicenter Prospective Study. Published online 2015. doi:10.1002/hep.28368

83. Poynard T, Bedossa P, Opolon P. Natural history of liver fibrosis progression in patients with chronic hepatitis C. The OBSVIRC, METAVIR, CLINIVIR, and DOSVIRC groups. *Lancet (London, England)*. 1997;349(9055):825-832. http://www.ncbi.nlm.nih.gov/pubmed/9121257

84. Prajapati K, Perez C, Rojas LBP, Burke B, Guevara-Patino JA. Functions of NKG2D in CD8+ T cells: an opportunity for immunotherapy. *Cell Mol Immunol*. 2018;15(5):470-479. doi:10.1038/cmi.2017.161

85. Quan Y, Thimme R, Zhang C, Tian Z, Zheng M. Liver-Mediated Adaptive Immune Tolerance. *Front Immunol | www.frontiersin.org*. 2019;10:2525. doi:10.3389/fimmu.2019.02525

86. Racanelli V, Rehermann B. The Liver as an Immunological Organ. Published online 2006. doi:10.1002/hep.21060

87. Rehermann B, Thimme R. Insights From Antiviral Therapy Into Immune Responses to Hepatitis B and C Virus Infection. *Gastroenterology*. 2019;156(2):369-383. doi:10.1053/j.gastro.2018.08.061

88. Reig M, Mariño Z, Perelló C, et al. *Unexpected High Rate of Early Tumor Recurrence in Patients with HCV-Related HCC Undergoing Interferon-Free Therapy Q*.

89. Rich NE, Murphy CC, Yopp AC, et al. Sex disparities in presentation and prognosis of 1110 patients with hepatocellular carcinoma. Published online 2020. doi:10.1111/apt.15917

90. Sagiv-Barfi I, Czerwinski DK, Levy S, et al. *Eradication of Spontaneous Malignancy by Local Immunotherapy*. Vol 10.; 2018. https://www.science.org

91. Salvoza NC, Giraudi PJ, Tiribelli C, Rosso N. Sex differences in non-alcoholic fatty liver disease: hints for future management of the disease. doi:10.37349/emed.2020.00005

92. Schinkel SCB, Carrasco-Medina L, Cooper CL, Crawley AM. Generalized liver- and blood-derived CD8+ T-Cell impairment in response to cytokines in chronic hepatitis C virus infection. *PLoS One*. 2016;11(6):1-18. doi:10.1371/journal.pone.0157055

93. Scholten D, Trebicka J, Liedtke C, Weiskirchen R. The carbon tetrachloride model in mice. Published online 2015. doi:10.1177/0023677215571192

94. Shah H, Bilodeau M, Burak KW, et al. The management of chronic hepatitis C: 2018 guideline update from the Canadian Association for the Study of the Liver. *CMAJ*. 2018;190(22):E677-E687. doi:10.1503/CMAJ.170453

95. Shen T, Zheng J, Liang H, et al. Characteristics and PD-1 expression of peripheral CD4+CD127loCD25hiFoxP3+ Treg cells in chronic HCV infected-patients. *Virol J 2011 81*. 2011;8(1):1-9. doi:10.1186/1743-422X-8-279

96. Shrivastava S, Steele R, Ray R, Ray RB. MicroRNAs: Role in hepatitis C virus pathogenesis. *Genes Dis*. 2015;2(1):35-45. doi:10.1016/j.gendis.2015.01.001

97. Shuai Z, Leung MW, He X, et al. Adaptive immunity in the liver. Published online 2016. doi:10.1038/cmi.2016.4

98. Stine JG, Wentworth BJ, Zimmet A, et al. Systematic review with meta-analysis: risk of hepatocellular carcinoma in non-alcoholic steatohepatitis without cirrhosis compared to other liver diseases. *Aliment Pharmacol Ther*. 2018;48(7):696-703. doi:10.1111/APT.14937

99. Sulava E, Bergin S, Long B, Koyfman A. Elevated Liver Enzymes: Emergency Department–Focused Management. *J Emerg Med*. 2017;52(5):654-667. doi:10.1016/j.jemermed.2016.10.016

100. Sutti S, Albano E. Adaptive immunity: an emerging player in the progression of NAFLD. *Nat Rev Gastroenterol Hepatol*. Published online 2020. doi:10.1038/s41575-019-0210-2

101. Swain M ARPKSGSATEMPEMBHECRH. Burden of nonalcoholic fatty liver disease in Canada, 2019–2030: a modelling study. Published online 2020. doi:10.9778/cmajo.20190212

102. Targher G, Corey KE, Byrne CD. NAFLD, and cardiovascular and cardiac diseases: Factors influencing risk, prediction and treatment. *Diabetes Metab*. 2021;47(2):101215. doi:10.1016/j.diabet.2020.101215

103. Thein H-H, Yi Q, Dore GJ, Krahn MD. Estimation of Stage-Specific Fibrosis Progression Rates in Chronic Hepatitis C Virus Infection: A Meta-Analysis and Meta-Regression. Published online 2008. doi:10.1002/hep.22375

104. Thimme R, Bukh J, Spangenberg HC, et al. *Viral and Immunological Determinants of Hepatitis C Virus Clearance, Persistence, and Disease*. www.pnas.org.

105. Tilg H, Moschen AR. Evolution of Inflammation in Nonalcoholic Fatty Liver Disease: The Multiple Parallel Hits Hypothesis. Published online 2010. doi:10.1002/hep.24001

106. Tobari M, Hashimoto E. Characteristic features of nonalcoholic fatty liver disease in Japan with a focus on the roles of age, sex and body mass index. *Gut Liver*. 2020;14(5):537-545. doi:10.5009/GNL19236

107. Tsochatzis EA, Bosch J, Burroughs AK. Liver cirrhosis. *Lancet*. 2014;383(9930):1749-1761. doi:10.1016/S0140-6736(14)60121-5

108. Urbani S, Amadei B, Tola D, et al. PD-1 Expression in Acute Hepatitis C Virus (HCV) Infection Is Associated with HCV-Specific CD8 Exhaustion. *J Virol*. 2006;80(22):11398-11403. doi:10.1128/JVI.01177-06

109. Valenti L, Bugianesi E, Pajvani U, Targher G. Nonalcoholic fatty liver disease: cause or consequence of type 2 diabetes? Published online 2016. doi:10.1111/liv.13185

110. Voskoboinik I, Whisstock JC, Trapani JA. Perforin and granzymes: function, dysfunction and human pathology. *Nat Publ Gr*. Published online 2015. doi:10.1038/nri3839

111. Vranjkovic A, Deonarine F, Kaka S, Angel JB, Cooper CL, Crawley AM. Direct-acting antiviral treatment of hcv infection does not resolve the dysfunction of circulating CD8+ T-cells in advanced liver disease. *Front Immunol*. 2019;10(AUG):1-18. doi:10.3389/fimmu.2019.01926

112. Wai C-T, Greenson JK, Fontana RJ, et al. A Simple Noninvasive Index Can

Predict Both Significant Fibrosis and Cirrhosis in Patients With Chronic Hepatitis C. Published online 2003. doi:10.1053/jhep.2003.50346

113. Walkin L, Herrick SE, Summers A, et al. *The Role of Mouse Strain Differences in the Susceptibility to Fibrosis: A Systematic Review*.; 2013. doi:10.1186/1755-1536-6-18

114. Wherry EJ. T cell exhaustion. *Nat Publ Gr*. Published online 2011. doi:10.1038/ni.2035

115. Wieland D, Kemming J, Schuch A, et al. TCF1+ hepatitis C virus-specific CD8+ T cells are maintained after cessation of chronic antigen stimulation. *Nat Commun*. 2017;8. doi:10.1038/ncomms15050

116. Xu S, Wang Y, Tai DCS, et al. QFibrosis: A fully-quantitative innovative method incorporating histological features to facilitate accurate fibrosis scoring in animal model and chronic hepatitis B patients. *J Hepatol*. 2014;61(2):260-269. doi:10.1016/j.jhep.2014.02.015

117. Yang D, Hanna DL, Usher J, et al. Impact of Sex on the Survival of Patients With Hepatocellular Carcinoma: A Surveillance, Epidemiology, and End Results Analysis. *Cancer*. 2014;120:3707-3723. doi:10.1002/cncr.28912

118. Yonkers NL, Sieg S, Rodriguez B, Anthony DD. Reduced naive CD4 T cell numbers and impaired induction of CD27 in response to T cell receptor stimulation reflect a state of immune activation in chronic hepatitis C virus infection. *J Infect Dis*. 2011;203(5):635-645. doi:10.1093/infdis/jiq101

119. Younossi Z, Anstee QM, Marietti M, et al. Global burden of NAFLD and NASH: Trends, predictions, risk factors and prevention. *Nat Rev Gastroenterol Hepatol*. 2018;15(1):11-20. doi:10.1038/nrgastro.2017.109

120. Younossi ZM, Koenig AB, Abdelatif D, Fazel Y, Henry L, Wymer M. Global Epidemiology of Nonalcoholic Fatty Liver Disease-Meta-Analytic Assessment of Prevalence, Incidence, and Outcomes. Published online 2015. doi:10.1002/hep.28431/suppinfo

121. Younossi ZM, Tampi RP, Racila A, et al. Economic and clinical burden of nonalcoholic steatohepatitis in patients with type 2 diabetes in the U.S. *Diabetes Care*. 2020;43(2):283-289. doi:10.2337/dc19-1113

122. Zheng C, Zheng L, Yoo J-K, et al. Landscape of Infiltrating T Cells in Liver Cancer Revealed by Single-Cell Sequencing. *Cell*. 2017;169(7):1342-1356.e16. doi:10.1016/j.cell.2017.05.035

123. Zhou Z, Xu M-J, Gao B. Hepatocytes: a key cell type for innate immunity. Published online 2016. doi:10.1038/cmi.2015.97;published